The Integration of sUAS into a Diverse Agricultural Operation

by

Andrew Newsum

B.S., Kansas State University, 2012

A THESIS

submitted in partial fulfillment of the requirements for the degree

MASTER OF SCIENCE

Department of Agronomy
College of Agriculture

KANSAS STATE UNIVERSITY
Manhattan, Kansas

2018

Approved by:

Major Professor
Dr. Antonio Ray Asebedo

Copyright

Abstract

Current population trends project that current agricultural production will need to increase by 110% by the year 2050 to support the growing worldwide population. Many agriculturalists are looking at precision agriculture technology to help achieve this production increase. One technology that is being heavily researched is the integration of small unmanned aerial systems (sUAS) and their sensors into the agricultural sector. Much research has already been conducted in the agronomic sector utilizing sUAS. However, relatively few advancements involving sUAS have been made in the animal science industry. This thesis focuses on how sUAS can be incorporated into a diverse cropping and livestock operation.

Chapter 1 - Evaluating Current Capabilities of sUAS and sUAS Mounted Sensors in Diverse Agricultural Operation: A Literature Review, focuses on the current capabilities of sUAS and explains how they are incorporated into cropping systems and livestock production.

Chapter 2 - Wheat Variety Interaction on Multispectral Based Vegetative Indices, focuses on wheat variety interaction with yield, grain protein content, NDVI, NDRE and CCCI. Ten wheat varieties were tested in large plot studies; yield, protein and multispectral data were collected for Feekes 4, 7, 10 and 10.5. Wheat variety was statically significant across all vegetative indices, protein and yield during less than favorable growing conditions.

Chapter 3 - Estimating Cattle Rectal Temperature Using Thermography, focuses on determining the ideal location for thermographic readings to be taken to predict rectal temperature of beef cattle. To establish if sUAS-based thermography could be utilized for cattle rectal temperature estimation, 35 crossbreed steers were selected and thermographic readings and rectal temperature data were collected and analyzed for correlation. This study found stronger relation in the animal's eye than other facial features.

Table of Contents

List of Figures

List of Tables

Acknowledgements

During my educational career, several individuals have supported my endeavors. First, I would like to recognize my major professor, Dr. Antonio Ray Asebedo. I first met Dr. Asebedo while working in the Kansas State University Polytech UAV lab. Dr. Asebedo had a meeting scheduled with the program head and my supervisor Mark Blanks. Mark was running a little late, so he told me there was “some ag guy” that he had scheduled a meeting with and needed me to keep him busy for a few minutes. That “ag guy” turned out to be Dr. Asebedo. While waiting for Mark, we talked for several minutes and really hit it off. During that conversation, Dr. Asebedo must have seen some potential in me, as he offered me a graduate research position the very next week. Dr. Asebedo has pushed me to follow my passion and explore new horizons. He has taught me the value of self-learning and to “ask Google” before you ask for help, as teachers will not always be around to explain things. I would also like to thank my committee members, Dr. Dale Blasi and Dr. Daniel Flippo, both of which have helped me to pursue my interests in cattle and in robotics. They were welcoming and offered me full use of their facilities and offered their expertise when I needed help. I would also like to acknowledge my fellow graduate students, Huan Wang and Ashely Laurence. Huan was truly a mentor and a friend, as he taught so many remote sensing and GIS techniques and brought delicious homemade Chinese food to the field for me to try. Ashley was a travel companion on long field work road trips, a study buddy for classes and a friend. I would also like to thank Victor Tomei and Scott Cain, our student workers, as they were extremely helpful. I would also like to express my gratitude to all the professors at Kansas State University for all the knowledge they bestowed upon me. Without all those listed above and the support they gave, I would have not been able to complete this Master’s degree.

Dedication

This thesis is dedicated to my friends and family, without whom I wouldn't have been able to complete this degree. A special dedication is due to my parents, Jeff and Ruth Ann Newsum. My parents have always believed in me and supported every dream I ever had. No matter what decision I made, good or bad, they were always there to support me and tell me they were proud of me. This unconditional support gave me the courage to try new things and learn new skills without the worry of being a disappointment or failing.

Chapter 1 - Evaluating Current Capabilities of sUAS and sUAS Mounted Sensors in Diverse Agricultural Operation: a Literature Review

Introduction

It is projected that crop production rates will need to increase by as much 110 percent from rates in 2005 to meet the projected demands of 2050 (Tilman et al. 2011). Increased demand for biofuels, population growth and the westernization of Asian diets all attribute to this projected demand (King et al. 2017; Pingali 2007; Foley et al. 2011). This increased demand will have to be met with increased production. Increased production will stem from high yielding crops and new technology resulting in more efficient agricultural practices. Small unmanned aerial vehicles (sUAS), more commonly referred to as drones, are one of said technologies that many are looking to improve yields.

According to the Federal Aviation Administration (FAA), a sUAS (small unmanned aircraft) is comprised of two main elements, UA (unmanned aircraft) and its associated controls and data links ("FAA 2016 Performance & Accountability Report," 2016). The FAA further defines a small UA as, "weighing less than 55 pounds, including everything that is onboard or otherwise attached to the aircraft, and can be flown without the possibility of direct human intervention from within or on the aircraft." Historically speaking, the first UA was invented in Greece in 425 B.C. while the first modern UA was later invented in WWII (Valavanis 2008). These first UAs had limited to no intelligence and were plagued with flight problems, causing them to be poorly adopted outside of military or recreational uses (Valavanis 2008). In recent years however, UAs have benefited from technological advances in battery, propulsion, micro-

processing and manufacturing techniques, making sUAS more obtainable and useful to the general public (Chao, Cao, and Chen 2010). With this increased adoption rate, more industries have become interested in using sUAS for remote sensing purposes. One of the most anticipated benefactors of sUAS based remote sensing is the agricultural industry. The Association of Unmanned Vehicles Systems International (AUVSI) estimated that from 2015 to 2025, American agriculture could see a 64-billion-dollar increase with the implementation of sUAS (AUVSI, 2013). This economic growth is attributed to not only an increase in jobs, but also an increase in agronomic yields (AUVSI, 2013).

It is important to realize that many American agriculturalists operate a diverse operation, producing both livestock and field crops. Therefore, it is important that sUAS technology be able to serve both the agronomic and the livestock sectors of production agriculture. Therefore, this paper will evaluate the current capabilities and agronomic impacts of sUAS and sUAS mounted sensors on diverse agricultural operations.

Current capabilities and uses of sUAS in diverse agricultural operations.

The agronomic sector has benefited from not only more numerous, but more successful sUAS based remote sensing research than the livestock production sector. This could be attributed to prevalence of precision agriculture and the remote sensing methods precision agronomists employed prior to the introduction of sUAS into the agronomic sector. In the 1960's and 1970's William Allen, David Gates, Harold Gausman and Jospeh Woolley built the foundation for remote sensing in agronomy, with their work correlating plant morphological properties with their spectral signatures in both the near-infrared and visible portions of the electromagnetic spectrum (Gates et al. 1965; Allen et al. 1969; Woolley 1971; Gausman, Allen,

and Escobar 1974; Gausman 1974; Gausman 1977). Their work in remote sensing has been the foundation for countless research and technological advances that allow agronomists to analyze spectral responses and quantify many agronomic parameters.

Remotely sensed high-throughput phenotyping is one such innovation. With the incorporation of a variety of sensors on UAVs and other autonomous vehicles, researchers now have the ability to non-invasive phenotype plants to gauge both physiological traits and resistance traits to both biotic and abiotic stresses in a timely manner (Singh et al. 2016). Broad scale phenotyping accelerates the acquisition of needed data so that breeders are able to select the most ideal progeny, increasing breeding efficiency(Araus and Cairns 2014; Lamsal, S. M. Welch, et al. 2017a; Lamsal, Stephen Welch, et al. 2017b).

This phenotyping ability has not only impacted breeding programs, it has also influenced several management decisions. sUAS remotely sensed thermal and multi-spectral data have been used in a variety of crops to detect water stress, (Baluja et al. 2012; Zarco-Tejada, González-Dugo, and Berni 2012; Gonzalez-Dugo et al. 2013; Zarco-Tejada et al. 2013). This increased ability to detect water stress allows producers to adjust in field water management strategies throughout the growing season (Gago et al. 2015). sUAS based remote sensing has also shown an ability to predict both yield potential and biomass (Wang 2017), leading to the ability to make in season nutrient management decisions (Lorence 2017). Weed management plans have also benefited from sUAS mounted sensors, as large scale weed scouting can be performed helping to identify proper herbicide and application rate (Rasmussen et al. 2013).

As previously stated, the animal science industry has had fewer sUAS based remote sensing research than the agronomic sector. However, sUAS based livestock products are starting to be developed. Researchers from the University of Tennessee concluded that UAV

retrofitted with RFID repeaters could be utilized to monitor cattle location and temperature when the cattle had the necessary thermometer equipped RFID tags (Webb, Mehlhorn, and Smartt 2017). UAV mounted thermal imagers have also been utilized to identify and count animals in tall grass (Israel 2011). Researchers are even looking to UAV teams to autonomously herd cattle from location to location (Jung and Ariyur 2017).

What sensors are currently used and what analytical information can be derived from the sequestered data?

The most important thing to realize when trying to incorporate sUAS into a diverse agricultural operation, is that the UAV is only a platform to carry a sensor payload and plays only a small role in the remote sensing process. The true analytical power is derived from the sensor payload used to gather raw data and the algorithms used to decipher and interpret this data. Thus, this paper will focus more on the sensor payloads and the data that can be interpolated from it. While there are numerous sensors available for integration into a sUAS platform, RGB (red, green, blue), multispectral and thermal imagers appear to be the most prevalent.

Similar to human eyes, RGB imagers work within the visual part of the radiometric spectrum and sense red, green and blue wavelengths. RGB cameras are without a doubt the most prevalent imager equipped on modern sUAS. In fact, most commercial off-the-shelf sUAS come equipped with a fully integrated RGB sensor. This has led some agronomists to research if these RGB cameras could be utilized to make agronomic decisions derived from their data. RGB imagers along with photogrammetry software has proven to be a reliable source to accurately predict plant height and biomass in maize and barley (Bendig et al. 2014; Li et al. 2016).

Research has also shown that RGB, imagery along with photogrammetric processes like structure from motion (SfM) computer visioning techniques, can be used to derive leaf area index ratings (Mathews and Jensen 2013).

Multispectral cameras

Multispectral imagers are another commonly used sensor, as these sensors have the ability to capture multiple spectral bands allowing for the creation of vegetative indices. While numerous vegetative indices have been created, this paper will discuss three, normalized difference vegetative index (NDRE), normalized differences red edge (NDRE) and canopy chlorophyll content index (CCCI).

NDVI

Normalized differences vegetative index or (NDVI) is a commonly used vegetative index used for agronomic purposes. The NDVI works on the basis that photosynthetic plant material can selectively absorb electromagnetic radiation, absorbing red (675nm) radiation and reflecting NIR (800nm) radiation (Jordan 1969). Prior to the formulation of NDVI, a simple ratio of 675 nm/800 nm reflectance values was utilized to detect relative greenness however, these values often had large errors when comparing location to location or cycle to cycle (Rouse et al.., 1974**)**. To combat the limitations of a simple ratio, Dr. J.W. Rouse and his colleagues developed the following normalized equation or vegetative index: $NDVI = \left(\frac{(\rho 800nm - \rho 670nm)}{(\rho 800nm + \rho 670nm)}\right)$, where ρ is equal to observed reflectance (Rouse et al., 1974). While originally developed for use with the broad banded ERTS-1 satellite, studies have indicated that a narrow band width of 15nm for both red and NIR bands are more optimal for vegetation monitoring (Thenkabail, Smith, Pauw, 2002,

Rouse et al., 1974). The center of these bandwidths vary from sensor to sensor and can be selected based on the desired observed vegetative trait. Thenkabail suggested two different band centers for the red portion of the electromagnetic spectrum (660nm and 675nm) and four centers (845nm, 905nm, 920nm, and 975nm) for the NIR portion of the electromagnetic spectrum (Thenkabail, Smith, and De Pauw 2002). Reflectance values in 660nm centered bands can be used to detect differences in plant biomass, leaf area index, cultivars and nitrogen and water stress in plants (Elvidge and Chen 1995; Carter 1998; Blackburn 1998). Whereas bands centered around 675nm have the highest crop-soil contrasts in the majority of crops throughout the majority of growing conditions (Thenkabail, Smith, and De Pauw 2002; Thenkabail, Smith, and De Pauw 1999). Bands centered around 845nm show a very strong correlation with total chlorophyll present (Schepers et al. 1996). 845nm is considered the "NIR shoulder" and using broad or narrow bands centered around the shoulder will result in very similar, if not overlapping reflectance values to narrower bands in the same range (Thenkabail, Smith, and De Pauw 2002). Therefore, with proper band center and width selection NDVI, can be used to estimate yield, biomass and N uptake (Stone et al., 1996; Tucker et al., 1980; Pinter et al., 1982). However, this estimation ability can be hampered by saturation effects throughout the growing season as LAI values change (Gitelson and Merzlyak 1996; Daughtry et al. 2000).

NDRE

Several years after the advent of NDVI, another commonly used vegetative index was developed; normalized difference vegetation index or NDRE. Similar to NDVI, NDRE also relies on a plant's selective absorption of electromagnetic radiation, however, NDRE utilizes the red edge portion of the spectrum (Barnes et al. 2000). NDRE can be calculated as follows:

$NDRE = \left(\frac{(\rho 800nm - \rho 720nm)}{(\rho 800nm + \rho 720nm)}\right)$, where ρ is the observed reflectance (Barnes et al., 2000). NDRE detects red-edge shifts throughout the growing season and throughout crop development (Thenkabail, Smith, and De Pauw 2002). Red-edge reflectance values reflect the chlorophyll content of plants, and research has shown while indirect, there is a high correlation between NDRE values and nitrogen content of crops (Tarpley, Reddy, and Sassenrath-Cole 2000).

CCCI

Even though strong correlations were observed between NDRE values and nitrogen content in crops (Tarpley, Reddy, and Sassenrath-Cole 2000) it becomes very difficult to do so when observing a diverse canopy as a whole (Fitzgerald et al. 2006). Fitzgerald gave a "cover problem" to prove this point, he explained that a sensor could sense the same amount of "green" in a crop with high cover and low nitrogen concentration as it would a crop with low cover and high nitrogen concentration (Fitzgerald et al. 2006). To overcome the previously described limitations of a single vegetative index, Barnes and his colleagues developed the canopy chlorophyll content index or CCCI (Barnes et al., 2000). The CCCI utilizes the upper and lower limits of NDRE as a function of NDVI's cover estimations to estimate canopy chlorophyll content (Barnes et al. 2000) and can be calculated as follows: $CCCI = \left(\frac{(NDRE - NDREmin)}{(NDREmax - NDREmin)}\right)$, where NDRE is the point of interest (Fitzgerald et al. 2006). This methods segregates vegetative signals from background signals (Fitzgerald et al. 2006) and thus areas of low chlorophyll content will have a CCCI value of 0 and areas of high chlorophyll content will have a value closer to 1 (Barnes et al. 2000). In summation, CCCI bridges that gap between NDVI's ability to predict crop cover rates and NDRE's ability to predict chlorophyll and indirectly predict nitrogen content of crops.

Infrared Thermography

Infrared thermography utilizes the fact that according to Planck's Law, all bodies with a temperature above absolute zero (-273°C) emit radiation and according to Wien's Law, all bodies with a temperature between -173°C and 2,727°C emit infrared radiation (Carlo 1995). Infrared thermal imagers are able to sense this infrared radiation and convert that information to a visible form.

While sUAS thermography has not been widely implemented in the animal science industry, handheld and ground based thermography has been incorporated in several research projects in the field of veterinary medicine. This is likely due to the fact that at high stocking densities, early identification of disease is expensive, time consuming and logistically challenging, yet is essential for proper treatment and control of contagious disease (Schaefer et al. 2004). However, many current practices utilize invasive procedures such as determining respiratory and heart rate, collecting blood samples and taking rectal temperatures (Stewart et al. 2008). The collection of these invasive measurements can cause skewed results as animals may exhibit anxiogenic responses during handling (Soerensen and Pedersen 2015). These factors have led researchers to try to develop non-invasive remotely sensed based procedures for identifying possible animal health concerns.

The use of thermal imagers and thermography are one such non-invasive procedure being tested for early disease diagnostics. One study showed that animals inoculated with bovine viral diarrhea virus (BVDV) show elevated ocular temperatures one day after inoculation, whereas conventional clinical exams did not identify BVDV symptoms for seven days after inoculation

(Schaefer et al. 2004). Ocular scans using thermographic sensors also showed a similar ability to detect early signs of bovine respiratory disease (Schaefer et al. 2007). By assessing blood flow in the coronary band using thermography, researchers have been able to detect foot lesions that can cause inflammation and lameness in cattle (Alsaaod et al. 2015). Seeing that symptoms of lameness only occur once lesions are severe (Laven and Proven 2000), the early recognition and treatment of these lesions is vital to minimize lameness symptoms (Leach et al. 2012). Thermographic sensors have even been identified as a good initial screening method for foot and mouth disease, based on lesion detection (Rainwater-Lovett et al. 2009). External parasites such as ticks have been identified and quantified on cattle using thermal imagers and computer based counting algorithms (Cortivo et al. 2016). While each study has produced research that has positively affected the animal science industry, the question still remains if these techniques could be adapted to an sUAS.

Summary

To meet the growing demand, the increased population of 2050 will require, agriculturalists will need to increase agronomic efficiency. To realize this efficiency increase, new production and management techniques will need to be designed and implemented. Many agriculturalists are looking to sUAS based remote sensing for this efficiency increase. Many strides have been made in the utilization of remote sensing in agronomic crops, using multispectral indices to quantify physiological differences. This ability of board scale phenotyping has increased agronomist's ability to better manage crops and breeder's ability to breed more ideal crop varieties. Unfortunately for diverse operators, the livestock industry has not enjoyed the same amount of success using sUAS, seeing relatively few sUAS technological

advancements. However, thermography has a proven track record of being useful in the detection of disease and other stress in cattle. These technological advancements in remote sensing will likely play a large role in production agriculture for years to come.

References

Allen, W. A., Gausman, H. W., Richardson, A. J., & Thomas, J. R. (1969). Interaction of isotropic light with a compact plant leaf. *JOSA*, *59*(10), 1376–1379.

Alsaaod, M., Schaefer, A. L., Büscher, W., & Steiner, A. (2015). The role of infrared thermography as a non-invasive tool for the detection of lameness in cattle. *Sensors*, *15*(6), 14513–14525.

Araus, J. L., & Cairns, J. E. (2014). Field high-throughput phenotyping: the new crop breeding frontier. *Trends in Plant Science*, *19*(1), 52–61.

AUVSI, 2013. The Economic Impact of Unmanned Aircraft Systems Integration in the UNited States. Retrieved February, 2017 form https://qzprod.files.wordpress.com/2013/03/econ_report_full2.pdf

Baluja, J., Diago, M. P., Balda, P., Zorer, R., Meggio, F., Morales, F., & Tardaguila, J. (2012). Assessment of vineyard water status variability by thermal and multispectral imagery using an unmanned aerial vehicle (UAV). *Irrigation Science*, *30*(6), 511–522. https://doi.org/10.1007/s00271-012-0382-9

Barnes, E. M., Clarke, T. R., Richards, S. E., Colaizzi, P. D., Haberland, J., Kostrzewski, M., … Thompson, T. (2000). Coincident detection of crop water stress, nitrogen status and canopy density using ground based multispectral data. In *Proceedings of the Fifth International*
Conference on Precision Agriculture, Bloomington, MN, USA (Vol. 1619).

Bendig, J., Bolten, A., Bennertz, S., Broscheit, J., Eichfuss, S., & Bareth, G. (2014). Estimating biomass of barley using crop surface models (CSMs) derived from UAV-based RGB imaging. *Remote Sensing*, *6*(11), 10395–10412.

Blackburn, G. A. (1998). Spectral indices for estimating photosynthetic pigment concentrations: a test using senescent tree leaves. *International Journal of Remote Sensing*, *19*(4), 657–675.

Carlo, A. D. (1995). Thermography and the possibilities for its applications in clinical and experimental dermatology. *Clinics in Dermatology*, *13*(4), 329–336. https://doi.org/10.1016/0738-081X(95)00073-O

Carter, G. A. (1998). Reflectance wavebands and indices for remote estimation of photosynthesis and stomatal conductance in pine canopies. *Remote Sensing of Environment*, *63*(1), 61–72.

Chao, H., Cao, Y., & Chen, Y. (2010). Autopilots for small unmanned aerial vehicles: a survey. *International Journal of Control, Automation and Systems*, *8*(1), 36–44.

Cortivo, P. D., Dias, E., Barcellos, J. O. J., Peripolli, V., Costa Jr, J. B. G., Dallago, B. S. L., & McManus, C. M. (2016). Use of thermographic images to detect external parasite load in cattle. *Computers and Electronics in Agriculture*, *127*, 413–417.

Daughtry, C. S. T., Walthall, C. L., Kim, M. S., De Colstoun, E. B., & McMurtrey Iii, J. E. (2000). Estimating corn leaf chlorophyll concentration from leaf and canopy reflectance. *Remote Sensing of Environment*, *74*(2), 229–239.

Elvidge, C. D., & Chen, Z. (1995). Comparison of broad-band and narrow-band red and near-infrared vegetation indices. *Remote Sensing of Environment*, *54*(1), 38–48.

FAA 2016 Performance & Accountability Report. (2016), 146.

Fitzgerald, G. J., Rodriguez, D., Christensen, L. K., Belford, R., Sadras, V. O., & Clarke, T. R. (2006). Spectral and thermal sensing for nitrogen and water status in rainfed and irrigated wheat environments. *Precision Agriculture*, *7*(4), 233–248.

Foley, J. A., Ramankutty, N., Brauman, K. A., Cassidy, E. S., Gerber, J. S., Johnston, M., …

West, P. C. (2011). Solutions for a cultivated planet. *Nature*, *478*(7369), 337.

Gago, J., Douthe, C., Coopman, Re., Gallego, Pp., Ribas-Carbo, M., Flexas, J., … Medrano, H. (2015). UAVs challenge to assess water stress for sustainable agriculture. *Agricultural Water Management*, *153*, 9–19.

Gates, D. M., Keegan, H. J., Schleter, J. C., & Weidner, V. R. (1965). Spectral properties of plants. *Applied Optics*, *4*(1), 11–20.

Gausman, H. W., Allen, W. A., & Escobar, D. E. (1974). Refractive index of plant cell walls. *Applied Optics*, *13*(1), 109–111.

Gausman, Harold W. (1974). Leaf reflectance of near-infrared. *Photogrammetric Engineering*, *40*(2).

Gausman, Harold W. (1977). Reflectance of leaf components. *Remote Sensing of Environment*, *6*(1), 1–9.

Gitelson, A. A., & Merzlyak, M. N. (1996). Signature analysis of leaf reflectance spectra: algorithm development for remote sensing of chlorophyll. *Journal of Plant Physiology*, *148*(3–4), 494–500.

Gonzalez-Dugo, V., Zarco-Tejada, P., Nicolás, E., Nortes, P. A., Alarcón, J. J., Intrigliolo, D. S., & Fereres, E. (2013). Using high resolution UAV thermal imagery to assess the variability in the water status of five fruit tree species within a commercial orchard. *Precision Agriculture*, *14*(6), 660–678.

Israel, M. (2011). A UAV-based Roe Deer Fawn Detection System. *International Archives of Photogrammetry and Remote Sensing, Vol XXXVIII-1/C22*, 1–5.

Jordan, C. F. (1969). Derivation of leaf-area index from quality of light on the forest floor. *Ecology*, *50*(4), 663–666.

Jung, S., & Ariyur, K. B. (2017). Strategic Cattle Roundup using Multiple Quadrotor UAVs. *International Journal of Aeronautical and Space Sciences*, *18*(2), 315–326.

King, T., Cole, M., Farber, J. M., Eisenbrand, G., Zabaras, D., Fox, E. M., & Hill, J. P. (2017). Food safety for food security: Relationship between global megatrends and developments in food safety. *Trends in Food Science & Technology*, *68*, 160–175.

Lamsal, A., Welch, S. M., Jones, J. W., Boote, K. J., Asebedo, A., Crain, J., … Arachchige, P. G. (2017a). Efficient crop model parameter estimation and site characterization using large breeding trial data sets. *Agricultural Systems*, *157*, 170–184. https://doi.org/10.1016/j.agsy.2017.07.016

Lamsal, A., Welch, S., White, J., Thorp, K., & Bello, N. (2017b). Problems with Estimating Anthesis Phenology Parameters in Zea mays: Consequences for Combining Ecophysiological Models with Genetics. *BioRxiv*, 087742.

Laven, R. A., & Proven, M. J. (2000). Use of an antibiotic footbath in the treatment of bovine digital dermatitis. *Veterinary Record*, *147*(18), 503–506. https://doi.org/10.1136/vr.147.18.503

Leach, K. A., Tisdall, D. A., Bell, N. J., Main, D. C. J., & Green, L. E. (2012). The effects of early treatment for hindlimb lameness in dairy cows on four commercial UK farms. *The Veterinary Journal*, *193*(3), 626–632. https://doi.org/10.1016/j.tvjl.2012.06.043

Li, W., Niu, Z., Chen, H., Li, D., Wu, M., & Zhao, W. (2016). Remote estimation of canopy height and above ground biomass of maize using high-resolution stereo images from a low-cost unmanned aerial vehicle system. *Ecological Indicators*, *67*, 637–648.

Lorence, A. A. (2017). *Evaluation of optical sensor technologies to optimize winter wheat (Triticum aestivum L.) management* (Thesis). Kansas State University. Retrieved from http://krex.k-state.edu/dspace/handle/2097/38245

Mathews, A. J., & Jensen, J. L. R. (2013). Visualizing and Quantifying Vineyard Canopy LAI Using an Unmanned Aerial Vehicle (UAV) Collected High Density Structure from Motion Point Cloud. *Remote Sensing*, *5*(5), 2164–2183. https://doi.org/10.3390/rs5052164

Pinter, P.J., Jr., R.D. Jackson, S.B. Idso, and R.J. Reginato (1981). Multidate spectral reflectance as predictors of yield in water stressed wheat and barley. Int. J. Remote Sens. 2:43-48.

Pingali, P. (2007). Westernization of Asian diets and the transformation of food systems: Implications for research and policy. *Food Policy*, *32*(3), 281–298.

Rainwater-Lovett, K., Pacheco, J. M., Packer, C., & Rodriguez, L. L. (2009). Detection of foot-and-mouth disease virus infected cattle using infrared thermography. *The Veterinary Journal*, *180*(3), 317–324. https://doi.org/10.1016/j.tvjl.2008.01.003

Rasmussen, J., Nielsen, J., Garcia-Ruiz, F., Christensen, S., & Streibig, J. C. (2013). Potential uses of small unmanned aircraft systems (UAS) in weed research. *Weed Research*, *53*(4), 242–248. https://doi.org/10.1111/wre.12026

Rouse, J.W., Jr., R.H. Haas, J.A. Schell, D.W. Deering, and J.C. Harlan. 1974. Monitoring the vernal advancement and retrogradation (greenwave Effect) of natural vegetation. Texas A&M Univ., College Station, TX. http://ntrs.nasa.gov/archive/nasa/casi.ntrs. nasa.gov/19750020419.pdf (accessed 1 Apr. 2015). SAS Institute. 2004.

Schaefer, A. L., Cook, N. J., Church, J. S., Basarab, J., Perry, B., Miller, C., & Tong, A. K. W. (2007). The use of infrared thermography as an early indicator of bovine respiratory disease complex in calves. *Research in Veterinary Science*, *83*(3), 376–384.

Schaefer, A. L., Cook, N., Tessaro, S. V., Deregt, D., Desroches, G., Dubeski, P. L., … Godson, D. L. (2004). Early detection and prediction of infection using infrared thermography. *Canadian Journal of Animal Science*, *84*(1), 73–80.

Schepers, J. S., Blackmer, T. M., Wilhelm, W. W., & Resende, M. (1996). Transmittance and reflectance measurements of cornleaves from plants with different nitrogen and water supply. *Journal of Plant Physiology*, *148*(5), 523–529.

Singh, A., Ganapathysubramanian, B., Singh, A. K., & Sarkar, S. (2016). Machine learning for high-throughput stress phenotyping in plants. *Trends in Plant Science*, *21*(2), 110–124.

Soerensen, D. D., & Pedersen, L. J. (2015). Infrared skin temperature measurements for monitoring health in pigs: a review. *Acta Veterinaria Scandinavica*, *57*, 5. https://doi.org/10.1186/s13028-015-0094-2

Soerensen, D. D., & Pedersen, L. J. (2015). Infrared skin temperature measurements for monitoring health in pigs: a review. *Acta Veterinaria Scandinavica*, *57*, 5. https://doi.org/10.1186/s13028-015-0094-2

Stewart, M., Stafford, K. J., Dowling, S. K., Schaefer, A. L., & Webster, J. R. (2008). Eye temperature and heart rate variability of calves disbudded with or without local anaesthetic. *Physiology & Behavior*, *93*(4), 789–797. https://doi.org/10.1016/j.physbeh.2007.11.044

Stone, M.L., J.B. Solie, W.R. Raun, R.W. Whitney, S.L. Taylor, and J.D. Ringer. (1996). Use of spectral radiance for correcting in-season fertilizer nitrogen deficiencies in winter wheat. Trans. ASAE 39:1623-1631.

Tarpley, L., Reddy, K. R., & Sassenrath-Cole, G. F. (2000). Reflectance indices with precision and accuracy in predicting cotton leaf nitrogen concentration. *Crop Science*, *40*(6), 1814–1819.

Thenkabail, P. S., Smith, R. B., & De Pauw, E. (1999). Hyperspectral vegetation indices for determining agricultural crop characteristics, CEO research publication series No. 1. *Center for Earth Observation, Yale University Press, New Haven*.

Thenkabail, Prasad S., Smith, R. B., & De Pauw, E. (2002). Evaluation of narrowband and broadband vegetation indices for determining optimal hyperspectral wavebands for agricultural crop characterization. *Photogrammetric Engineering and Remote Sensing*, *68*(6), 607–622.

Tilman, D., Balzer, C., Hill, J., & Befort, B. L. (2011). Global food demand and the sustainable intensification of agriculture. *Proceedings of the National Academy of Sciences*, *108*(50), 20260–20264.

Tucker, C.J., J.H. Elgin, Jr., and J.E. McMurtry III. (1980). Relationship of spectral data to grain yield variation. Photogrammetric Eng. Remote Sens. 46:657-666.

Valavanis, K. P. (2008). *Advances in unmanned aerial vehicles: state of the art and the road to autonomy* (Vol. 33). Springer Science & Business Media.

Wang, H. (2017). Crop assessment and monitoring using optical sensors. Retrieved from http://krex.k-state.edu/dspace/handle/2097/38224

Webb, P., Mehlhorn, S. A., & Smartt, P. (2017). Developing Protocols for Using a UAV to Monitor Herd Health. In *2017 ASABE Annual International Meeting* (p. 1). American Society of Agricultural and Biological Engineers.

Woolley, J. T. (1971). Reflectance and transmittance of light by leaves. *Plant Physiology*, *47*(5), 656–662.

Zarco-Tejada, P. J., González-Dugo, V., Williams, L. E., Suárez, L., Berni, J. A. J., Goldhamer, D., & Fereres, E. (2013). A PRI-based water stress index combining structural and chlorophyll effects: Assessment using diurnal narrow-band airborne imagery and the CWSI thermal index. *Remote Sensing of Environment*, *138*, 38–50. https://doi.org/10.1016/j.rse.2013.07.024

Zarco-Tejada, Pablo J., González-Dugo, V., & Berni, J. A. (2012). Fluorescence, temperature and narrow-band indices acquired from a UAV platform for water stress detection using a micro-hyperspectral imager and a thermal camera. *Remote Sensing of Environment*, *117*, 322–337.

Chapter 2 - Wheat Variety Interaction on Multispectral Based Vegetative Indices.

Abstract

Remote sensing vegetative indices are quickly becoming a widely adopted tool for both research and production agricultural. Of these vegetative indices, NDVI, NDRE and CCCI are among the most commonly utilized. Several studies have shown that these indices, along with complex algorithms can be utilized for nutrient recommendations, biomass estimations, yield estimations and numerous other agronomic benefits. This study looks at what interactions, if any, wheat variety has on vegetative indices, yield and grain protein content. Trials were established in Gypsum, Kansas in 2016 and 2017. In 2016, seven varieties of wheat (Everest, WB Cedar, SY Wolf, 1863, SY Monument, WB 4458 and Hotrod) were planted in 9 meters by 243 meters strips, with two replications of each variety. In 2017, five varieties of wheat (Everest, 1863, WB 4269, WB Grainfield and SY Gallant) were planted in 21 meters by 274 meters strips, with two replications of each variety. These fields were then monitored using a Micasense RedEdge® multispectral imager carried by a DJI s1000 and DJI Matrice. sUAS data was collected on a biweekly basis by flying the field at 121 meters agl with 80 percent overlap collecting data in the blue, green, red, red edge and near-infrared portion of the electromagnetic spectrum. This multispectral data was then processed and NDVI, NDRE and CCCI values were calculated for each plot. After statistical analysis, it was observed that during 2016 there was no statistical difference between the interaction of wheat variety and yield, however in 2017 a statistical difference was observed. This study also found a statistical difference between variety and vegetation indices throughout the growing season during key growth stages.

Introduction

To meet the ever increasing demand for agricultural products, producers and breeders have looked for a better method to phenotype their crops. Traditional phenotyping is often done by scouting the field on foot and is very time consuming and labor intensive. Due to the time consuming nature of traditional in-field phenotyping, it is very hard for wide scale inspection of crops, and slowing genetic and agronomic technologic progress. In the 1960s and 1970s agronomists started researching how optic based remote sensing techniques could be incorporated into the agronomic sector to help modernize the plant phenotyping process. These remote sensing techniques led not only to increased scouting efficiency, but also granted the ability to recognize plant physiological traits invisible to the human eye. William Allen, David Gates, Harold Gausman and Jospeh Woolley laid the foundation for agronomic remote sensing by correlating plant morphological properties with their spectral signatures in both the near-infrared and visible portions of the electromagnetic spectrum (Allen, Gausman, Richardson, & Thomas, 1969; Gates, Keegan, Schleter, & Weidner, 1965; Gausman, 1974, 1977; Woolley, 1971). This foundational work relies heavily on the fact that, photosynthetic plant material selectively absorbs and reflects portions of the electromagnetic spectrum (Jordan, 1969). Using this knowledge several plant vegetative indices were developed to quantify plant physiological and morphological traits in vegetation.

Until recently, even with all the benefits these phenotyping measures could provide, many agronomists failed to incorporate remote sensing into their operations. This is likely due to many of the early remote sensing operations being carried out using satellites with low temporal and spatial resolution or by manned aircraft, which could be costly to operate. However, with the advent of inexpensive commercially available small unmanned aerial systems (sUAS) and

optical sensors, many agronomists are showing interest in the utilization and incorporation of remote sensing based phenotyping. These inexpensive sUAS and inexpensive sUAS based sensors have allowed for agronomists to collect remotely sensed data without having to consider satellite return times or satellite band selection. This allows agronomists to cost effectively monitor crops throughout the growing season with high temporal and high spatial data. With this increased phenotypic data set, agronomists have been better able to select agronomic practice and genetic lines. These phenotyping methods showed an ability to predict yield and biomass (Wang, 2017), make fertilizer recommendations (Lorence, 2017), create weed management plans (Rasmussen, Nielsen, Garcia-Ruiz, Christensen, & Streibig, 2013) and numerous other agronomic processes.

Vegetative Indices

Many of these advancements have utilized sUAS based multispectral imagers and the vegetative indices calculated from their data. While numerous vegetative indices have been derived for both satellite based sensors and aerial based sensors, NDVI, NDRE and CCCI are among the most common.

NDVI

Perhaps the most widely recognized vegetative index, normalized difference vegetation index (NDVI) depends on the plants ability to selectively absorb red light (650nm) and reflect near infrared light (800nm) (Jordan, 1969). In 1973, Dr. John Rouse utilized this physiological trait to formulate the NDVI as follows $NDVI = \left(\frac{(\rho 800nm - \rho 670nm)}{(\rho 800nm + \rho 670nm)}\right)$, where ρ is equal to observed reflectance (Rouse Jr, 1973). These bands were originally selected for the broad bands of the ERTS-1, but more recent studies have indicated that bands of 15nm are more ideal for vegetative monitoring (Rouse Jr, 1973; Thenkabail, Smith, & De Pauw, 2002). By properly selecting the

center of these narrow bands, we can differentiate plant traits. Bands centered around 660nm will detect changes in plant biomass, leaf area index and nitrogen and drought stress in plants (Blackburn, 1998; Elvidge & Chen, 1995), whereas bands centered around 675nm have a greater plant to soil contrast (Thenkabail et al., 2002). With proper band selection, NDVI can be utilized to estimate yield, nitrogen uptake and biomass (Pinter Jr, Jackson, Idso, & Reginato, 1981; Stone et al., 1996; Tucker, Holben, Elgin Jr, & McMurtrey III, 1980). However, these estimation abilities are greatly limited by saturation effects in areas of high leaf area index (Daughtry, Walthall, Kim, De Colstoun, & McMurtrey Iii, 2000; Gitelson & Merzlyak, 1996).

NDRE

To help combat the saturated driven shortcomings of NDVI, normalized difference red-edge was created. Much like NDVI, NDRE also relies on a plant's ability to selectively absorb radiation, however NDRE utilizes the red-edge (720nm) portion of the electromagnetic spectrum and is formulated $NDRE = \left(\frac{(\rho 800nm - \rho 720nm)}{(\rho 800nm + \rho 720nm)}\right)$, where ρ is observed reflectance (Barnes et al., 2000). By utilizing the red-edge, NDRE can gauge chlorophyll content and indirectly gauge nitrogen content of plants (Tarpley, Reddy, & Sassenrath-Cole, 2000). However, in a diverse canopy this ability can be limited; the same sensor may see the same amount of "green" in areas of high nitrogen concentration and low cover as it would in areas of low nitrogen concentration and high cover (Fitzgerald et al., 2006).

CCCI

The canopy chlorophyll content index CCCI was designed to alleviate some of these cover issues. The CCCI is formulated by $CCCI = \left(\frac{(NDRE - NDREmin)}{(NDREmax - NDREmin)}\right)$, where NDRE is the point of interest (Barnes et al., 2000) and utilizes the upper and lower limits of NDRE as a

function of NDVI to segregate vegetation signals from background signals (Fitzgerald et al., 2006). Using this calculation, CCCI will value the area of highest chlorophyll content close to 1 and areas of low chlorophyll content closer to zero (Barnes et al., 2000). With this formulation, CCCI is able to use NDVI's ability to predict cover rates and NDRE's ability to predict chlorophyll.

Rational and objectives

As previously discussed, agronomists are continuously striving to improve plant genetics and agronomic practices. Many agronomists are utilizing sUAS based vegetative indices to phenotype their crops. However, many studies will only utilize one variety, choosing to focus on other variables. The objective of this study was to determine if wheat variety impacts yield, protein, and NDVI, NDRE and CCCI values. This is important if broad scale phenotyping is to be successful. This will also help determine if variety interactions should be considered when developing vegetative index drive agronomic algorithms.

Materials and Methods

Sight selection and experimental design.

The study was conducted over two growing seasons in 2015-2016 and 2016-2017, in cooperation with Justin Knopf a local producer. Sites were located in Saline County, Kansas, near the town of Gypsum. Sites were selected to accommodate this study's large physical size. Soil textural and drainage properties were acquired from the NRCS's Web Soil Survey webb application.

Gypsum 2016

In 2016, trials were established in Gypsum, Kansas in a field located near 38°42'35.1"N 97°26'19.4"W. This slightly sloped field contained soil classified as 74.8% Hord silt loam and 26.2% Longford silt loam. This field was then split into fourteen, 9 meters x 243 meters trial plots with ground control points (GCPs) at each corner. These plots were then randomly assigned one of the following wheat varieties: Everest, 1863, Hotrod, WB Cedar, WB 4458, SY Wolf and SY Monument. Each variety was planted in two replications. These large plot dimensions were chosen to capture variability throughout the field and also so satellite data could be extracted for each plot for subsequent research.

Gypsum 2017

In 2017, trials were establish once again in Gypsum, Kansas, however a larger field was utilized, located near 38°43'35.0"N 97°26'33.7"W. This slightly sloped field was classified as 81.9% Longford silt loam, 16.6% Detroit silty clay loam and 1.5% Crete silt loam. This field was divided into ten, 21 meters by 274 meter trial plots with ground control points (GCPs) at each corner. These plots were then randomly assigned one of the following wheat varieties: Everest, 1863, WB 4269, WB Grainfield, SY Gallant. Each variety was planted in two replications. Plot width was doubled this year to increase the likelihood of having satellite pixels only encompass a single variety. Total variety numbers were changed from seven varieties to five varieties to accommodate field size limitations.

Variety Selection and management.

Wheat varieties were selected with consultation from seed providers and extension agents, to reflect popularly planted wheat varieties and the new upcoming varieties. All wheat management decisions including seeding rate, nutrient management, weed management and fungicide applications, were uniform across the trial and were determined by the producer.

Data Collection

UAVs

Three aircrafts were used during this study. In the 2015-2016 growing year, a DJI s800 evo hexacopter equipped with a DJI A2 flight controller was used until being replaced by the larger DJI s1000 octocopter also equipped with a DJI A2 flight controller for data collection. The s1000 was selected to replace the s800 due to its larger payload capacity and increased flight endurance. Both aircraft utilized the same flight controller, telemetry links, ground station and sensor payload. During the 2016-2017 growing year, a DJI Matrice quadcopter was selected for data acquisition, for its smaller physical size, ease of operation and increased endurance. Even with the change in aircraft, data quality and acquisition techniques remained the same across all platforms. DJI ground station software and Maps Made Easy Map Pilots V2.0 IOS based mobile application was utilized for flight planning an automatization.

Sensor payloads

Due to the aircraft being used in multiple studies, sensor payloads varied from aircraft to aircraft, however the sensor used in this study, the MicaSense RedEdge, remained constant across all years and aircraft. The s800 and s1000 carried a Cannon T4i RGB camera and the Matrice was equipped with a DJI X3, 12-megapixel RGB camera and FLIR Vue Pro R. These cameras were not utilized in this study. However, all three aircrafts carried a MicaSense RedEdge multispectral camera equipped with a downwelling light sensor (DLS) and an external 3DR brand GPS module. The RedEdge multispectral sensor has 5 individual cameras allowing it to collect the following bands individually:

Band Name	Band Center (nm)	Bandwidth FWHM (nm)
Blue	475	20
Green	560	20
Red	668	10
Red-edge	717	10
Near IR	840	10

Table 2-1 MicaSense RedEdge Band Description

Data Acquisition

Data was collection was conducted under certificate of authorization number 2014-CSA-6-COA and later under FAA part 107 regulations. All flights were conducted under the supervision of a licensed pilot and remote pilot in command. Data was collected at 121 meter above ground level, with 80 percent fore and side overlap, within two and one half hours of solar noon. Data was collected on a weekly basis to allow the capture of key growth stages. Great care was taken to only collect data when sky conditions were consistent, meaning full sun or full overcast. If lighting conditions did vary during data collection, that data was culled and not utilized for analysis. Calibration images were taken before and after data collection flights utilizing a MicaSense RedEdge Calibration panel. Yield data was collected from a Case 7130 combine equipped with a voyager 3 yield monitor that was calibrated before harvesting.

Data processing and interpolation

Raw data from the MicaSense RedEdge was uploaded to MicaSense Atlas cloud based analytics application for both calibration and orthomosaic construction. Once processed, orthomosaic tif files were imported into ArcGis ArcMap 10.5 for data analysis. All orthomosaic were georeferenced to the initial flight using GCPs placed in the field. Once georeferenced,

NDVI, NDRE and CCCI maps were made for each flight. This data was monitored and processed after every flight, and mean VI values were collected for each research plot. Yield monitor information was also imported into ArcMap, kriged and quantified for each plot.

Statistical analysis procedure

After collection of vegetation index values, yield values and grain protein, SAS 9.2 statistical software was utilized for analysis. Using a PROC GLIMMIX model and Tukey test, alpha 0.05, with variety as treatment and dependent variables as yield, grain protein, NDVI, NDRE and CCCI. The vegetative indices; NDVI, NDRE and CCCI were tested at Feekes 4, Feekes 7, Feekes 10 and Feekes 10.5. After statistical analysis, statistical graphs were made in Microsoft Excel 2016.

Results and Discussion

Yield and Protein 2016 & 2017

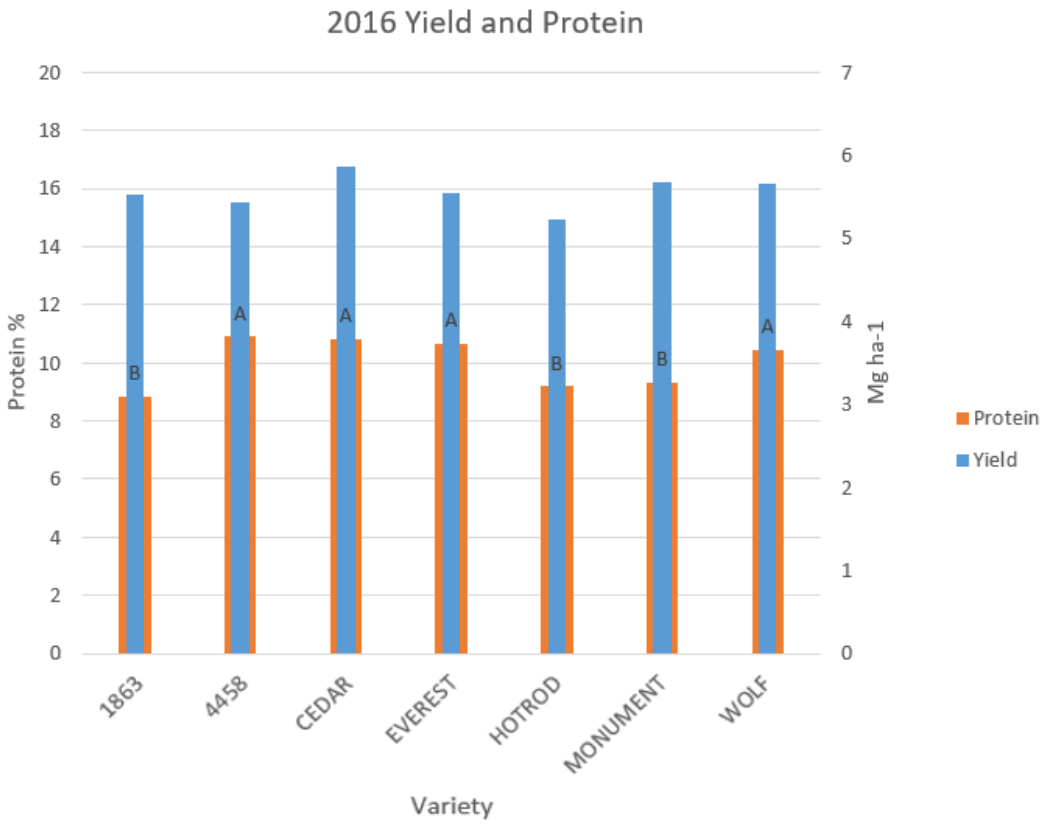

Figure 2-1 2016 yield (Pr>F 0.1408) and protein (Pr>F <0.0001)

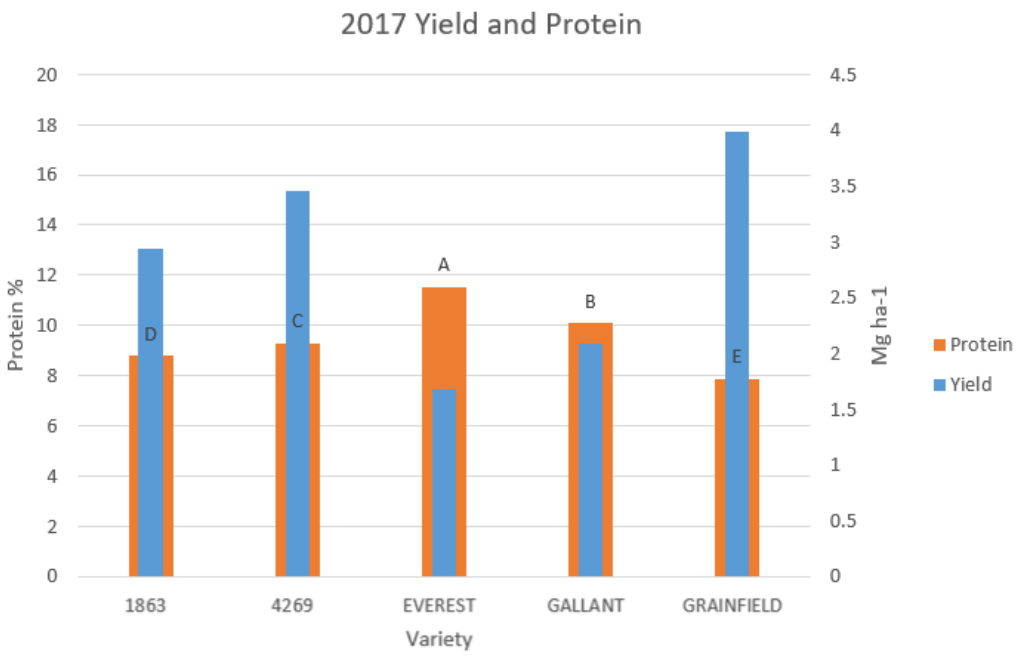

Figure 2-2 2016 yield (Pr>F <0.0001) and protein (Pr>F <0.0001)

This study found that during the 2016 growing year, the tested varieties had no impact on yield (Pr>F 0.1408), however, in the 2017 growing year, variety did have a statistical impact on yield (Pr>F <0.001). These results are likely due the varieties interaction with the growing environment. The 2016 growing season was an exceptionally favorable year for wheat production with more precipitation and less foliar stresses. These favorable growing conditions likely masked some of the variety traits making all varieties yield statistically the same. The 2017 growing season was a far less conducive to wheat production. 2017 was a drier, year with less precipitation and more foliar issues in the form of Wheat Streak Mosaic. These less than ideal growing conditions, along with differing variety traits allowed some varieties to statistically out perform their competitors in the form of grain yield.

This research found similar results when comparing variety interaction with grain protein. While both years saw grain protein contents statistically different across varieties, more variation

was found in the 2017 growing season with 5 statistical groupings, compared to the 2016 growing with season 2 statistical groupings. These results can once again be explained by the varieties' interaction with the growing environment in which they were produced. Variety traits were more visible in times of stress than in conducive environments.

Feekes 4 2016 & 2017

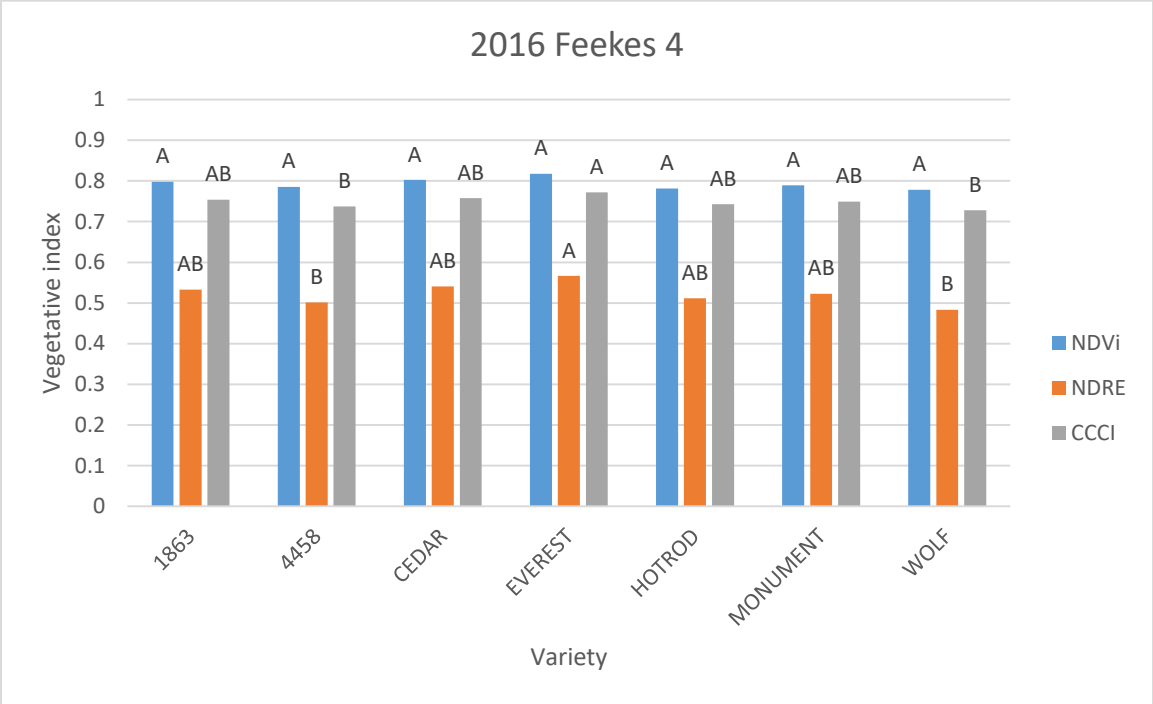

Figure 2-3 2016 Feekes 4: NDVI (Pr>F 0.1684), NDRE (Pr>F 0.0051) and CCCI (Pr>F 0.0052)

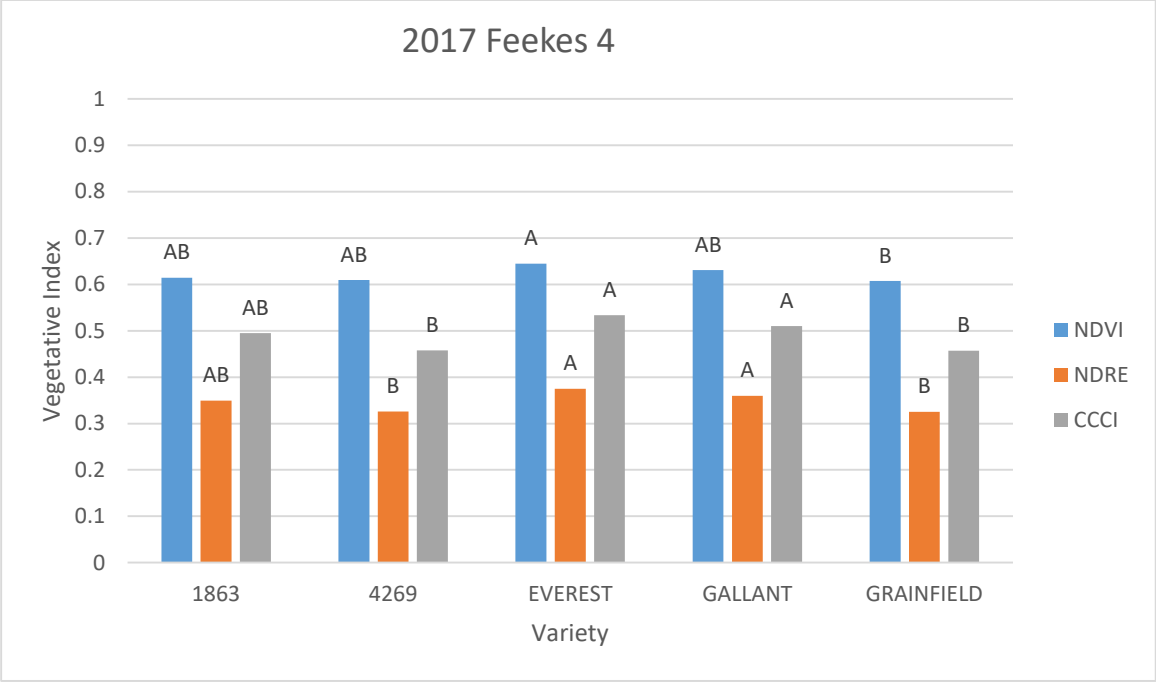

Figure 2-4 2017 Feekes 4: NDVI (Pr>F <0.0192), NDRE (Pr>F <0.001) and CCCI (Pr>F<0.001)

Variety trait differences were also observed in all vegetative indices, across all growth stages except for the NDVI reading taken at Feekes 4 in 2016. This research found that NDVI readings at Feekes 4 in 2016 was not statistically significant (Pr>F 0.1684) across varieties. Once again this can mostly be attributed to environmental factors. As previously stated, 2016 had very conducive weather and therefore the varieties had similar tillering rates and biomass. NDVI, while well suited for biomass detection, was unable to statistically separate these varieties due to their similar tillering. However, NDVI reading at Feekes 4 in 2017 were statically different as variety environmental interactions were present. In 2016, both NDRE and CCCI showed statistical differences across varieties, when NDVI did not. This is due to what the vegetative indices are targeting. While NDVI is a good predictor of biomass, NDRE and CCCI are better predictors of chlorophyll. This explains why we see a statistical difference in NDRE and CCCI

values and not in NDVI values. While the varieties in 2016 all had similar biomasses, some varieties had higher chlorophyll content than others. The stressful environment in the 2017 growing season allowed for variety traits to be observed in both NDRE and CCCI vegetative indices.

Feekes 7 2016 & 2017

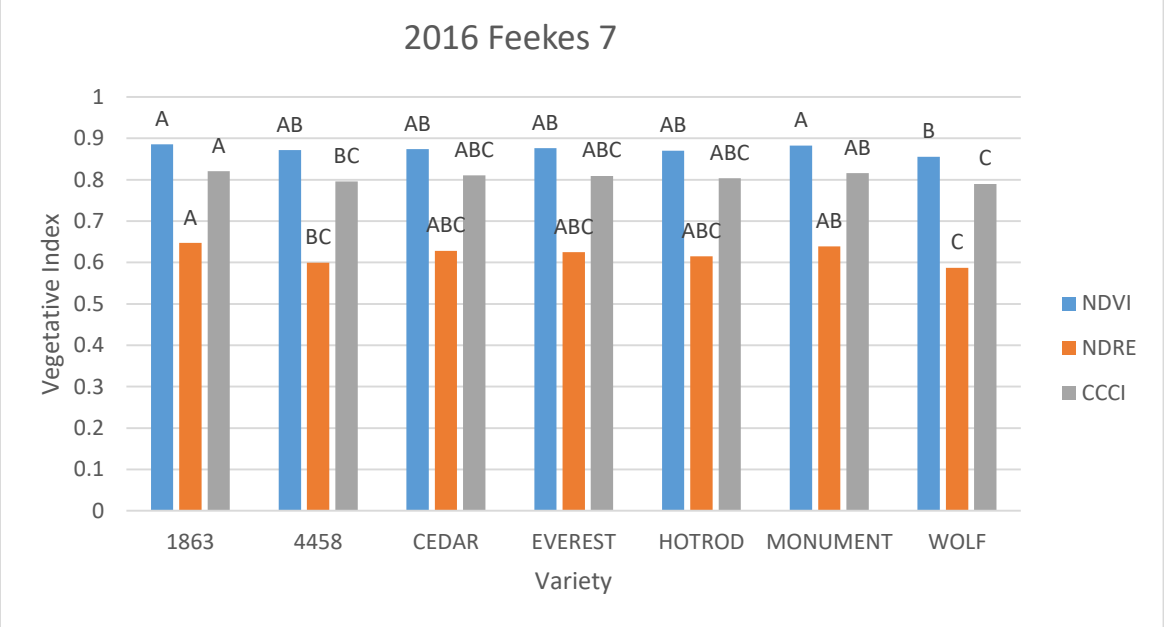

Figure 2-5 2016 Feekes 7: NDVI (Pr>F 0.0292), NDRE (Pr>F 0.0006) and CCCI (Pr>F 0.0006)

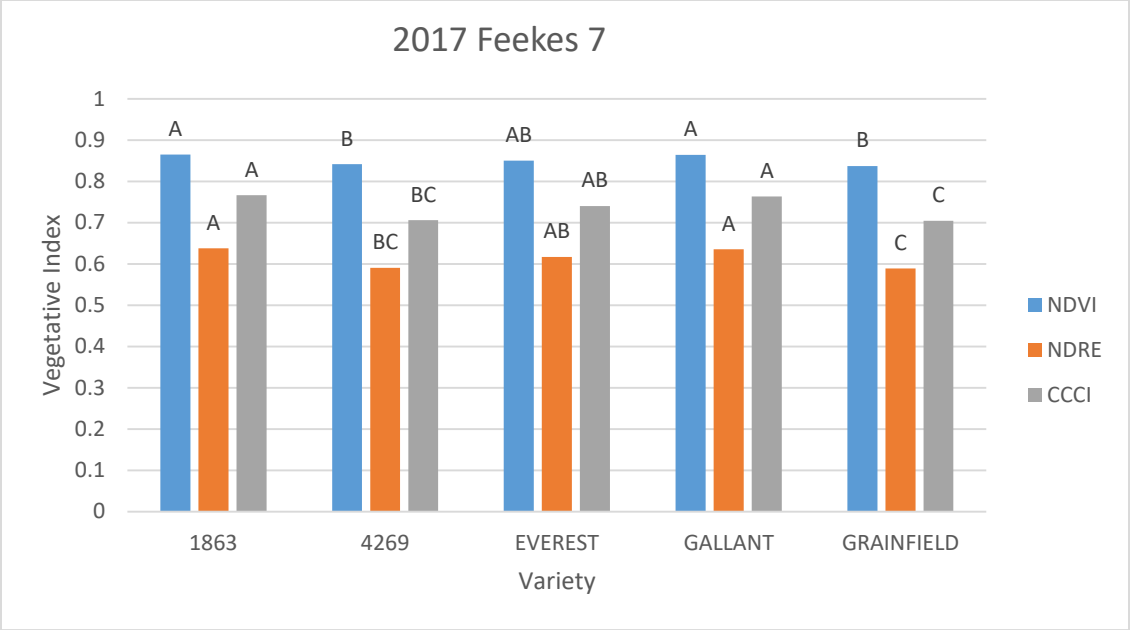

Figure 2-6 2017 Feekes 7: NDVI (Pr>F <0.001), NDRE (Pr>F <0.001) and CCCI (Pr>F <0.001)

Similar to earlier growth stages, variety interactions were observed and statistically significant across both years and all vegetative indices. Unlike Feekes 4 in 2016, NDVI values were statistically significant in Feekes 7, as biomass accumulation levels started differing with variety traits. In both the 2016 and 2017 growing seasons, more variation across varieties was observed in the two vegetative indices using the red-edge portion of the spectrum, NDRE and CCCI, than the red based NDVI.

Feekes 10 2016 & 2017

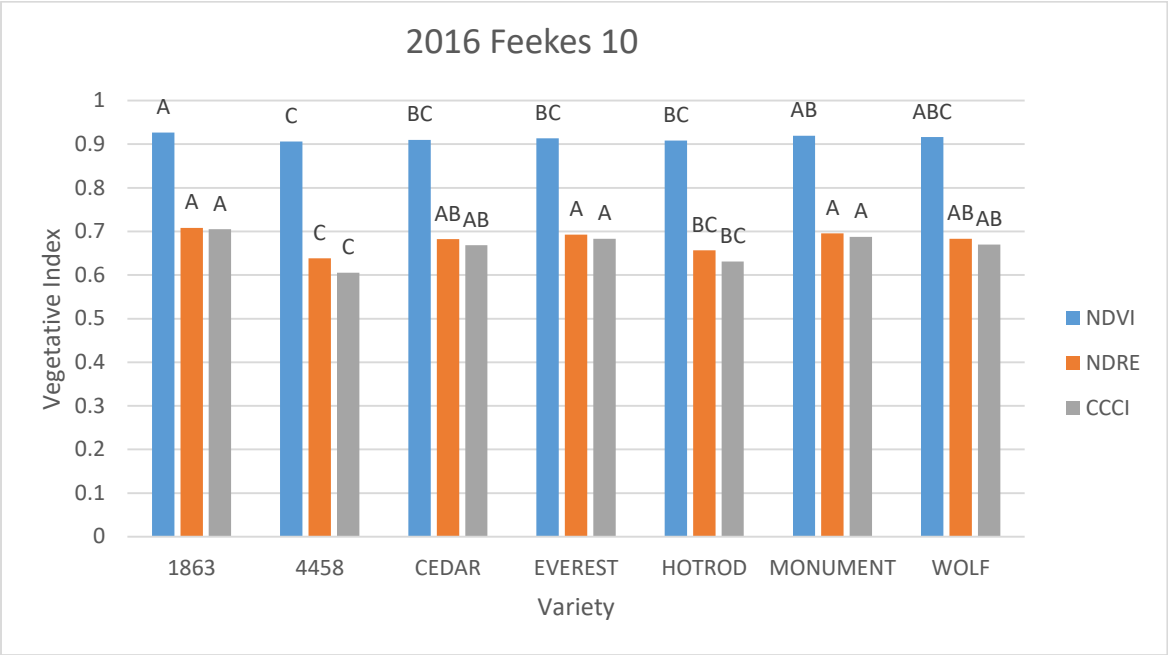

Figure 2-7 2016 Feekes 10: NDVI (Pr>F <0.001), NDRE (Pr>F <0.001) and CCCI (Pr>F <0.001)

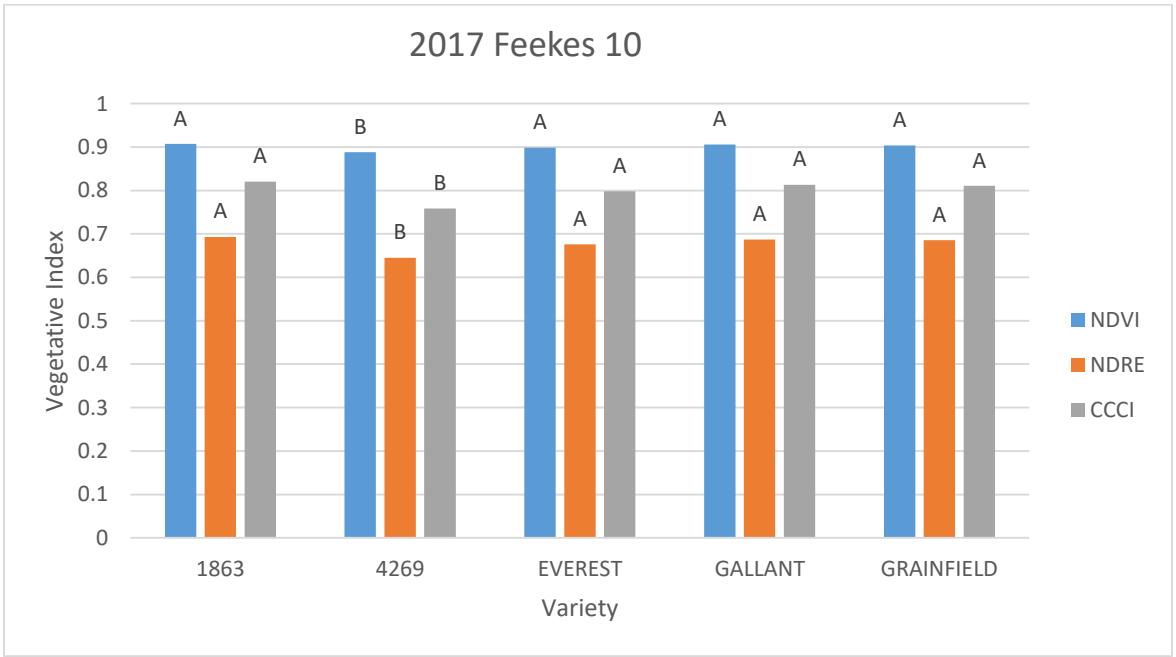

Figure 2-8 2017 Feekes 10: NDVI (Pr>F <0.001), NDRE (Pr>F <0.001) and CCCI (Pr>F <0.001)

Feekes 10 showed variety differences during both years across all vegetative indices. The 2017 growing season provided interesting results in NDRE and CCCI indices. The 2017 growing season saw several foliar stresses, including wheat streak mosaic. Looking back to Feekes 7 in 2017 figure (2-6), we see that two wheat varieties, 4269 and Grainfield are both performing poorly compared to the other varieties. While this is evident in NDVI, NDRE and CCCI are able to recognize more differentiation between varieties. However, when comparing these same varieties in Feekes 10, it is evident that Grainfield's NDRE and CCCI values are starting to rise, while 4269's values remain low.

Feekes 10.5 2016 & 2017

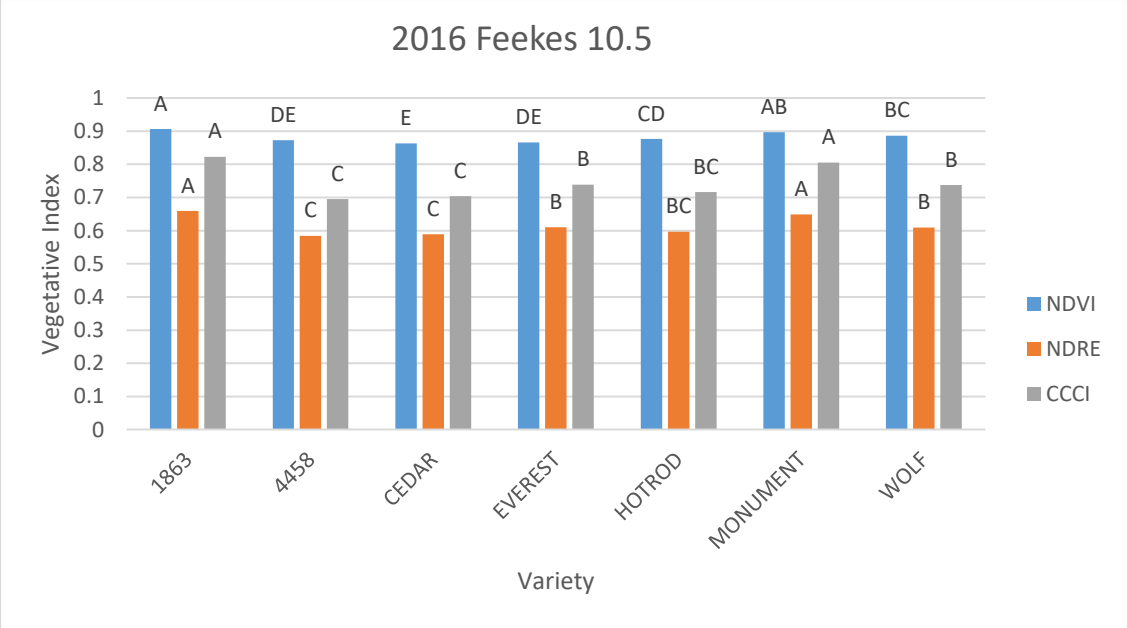

Figure 2-9 2016 Feekes 10.5: NDVI (Pr>F <0.001), NDRE (Pr>F <0.001) and CCCI (Pr>F <0.001)

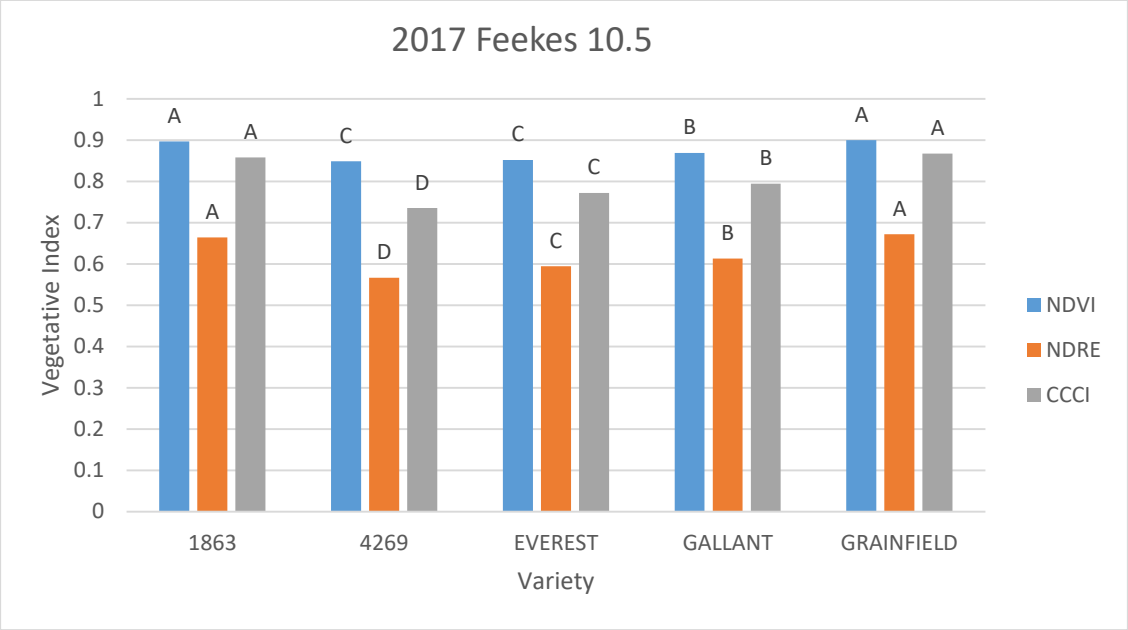

Figure 2-10 2017 Feekes 10.5: NDVI (Pr>F <0.001), NDRE (Pr>F <0.001) and CCCI (Pr>F <0.001)

Feekes 10.5 also showed statistical differences across all varieties and indices for both years. Already in Feekes 10.5 we can start to see variety differences in maturation rates. A prime example of this is comparing 1863, a late maturing variety, to Everest, an early maturing variety. Both varieties had similar vegetative indices readings in Feekes 7 and 10, however their difference in maturation rate is evident in Feekes 10.5. The earlier maturing Everest is seeing declining vegetative indices readings as head development and nitrogen translocation occurs, whereas, the slowing maturing 1863 does not see these declines.

Vegetation Indices Yield Predictions

NDVI	F4	F7	F10	F105
1863	0.0217	0.105	0.5791	0.2625
4458	0.0635	0.0376	0.2738	0.2248
Cedar	0.0823	0.0004	0.5364	0.3864
Everest	0.2897	0.4968	0.8859	0.8389
Hot Rod	0.0027	0.3233	0.871	0.7895
Monument	0.3228	0.3223	0.1835	0.0235
Wolf	0.6286	0.7318	0.535	0.2343
All	0.0286	0.1525	0.6306	0.5256

Table 2-2 Yield/NDVI 2016 r^2

NDRE	F4	F7	F10	F105
1863	<0.0001	0.2728	0.1784	0.1984
4458	0.0431	0.0003	0.0194	0.0239
Cedar	0.2675	0.0184	0.3979	0.2829
Everest	0.2067	0.5111	0.8297	0.9164
Hot Rod	0.1584	0.2032	0.0814	0.7919
Monument	0.3871	0.4264	0.1532	0.3191
Wolf	0.604	0.8379	0.512	0.5847
All	0.0011	0.1495	0.0538	0.3117

Table 2-3 Yield/NDRE 2016 r^2

CCCI	F4	F7	F10	F105
1863	<0.0001	0.2728	0.1792	0.1994
4458	0.0431	0.0003	0.0199	0.0242
Cedar	0.2973	0.0184	0.3977	0.2846
Everest	0.208	0.5111	0.8295	0.916
Hot Rod	0.1578	0.2032	0.0816	0.7918
Monument	0.3874	0.4264	0.1538	0.3217
Wolf	0.6034	0.8379	0.5122	0.5858
All	0.0011	0.1495	0.054	0.311

Table 2-4 Yield/CCCI 2016 r^2

NDVI	F4	F7	F10	F10.5
1863	0.1734	0.0009	0.0794	0.8116
4269	0.0151	0.0233	0.3357	0.4861
Everest	0.0007	0.0052	0.1185	0.4463
Gallant	0.0042	0.1984	0.3688	0.7269
Grainfield	0.0117	0.0557	0.0002	0.2778
All	0.1752	0.0631	0.0006	0.2642

Table 2-5 Yield/NDVI 2017 r^2

NDRE	F4	F7	F10	F10.5
1863	0.02895	0.0101	0.027	0.7184
4269	0.0468	0.0879	0.1959	0.5043
Everest	0.0092	0.0497	0.1592	0.2132
Gallant	0.0014	0.0837	0.1353	0.7352
Grainfield	0.0066	0.0092	0.092	0.2415
All	0.3425	0.1387	0.0069	0.164

Table 2-6 Yield/NDRE 2017 r^2

CCCI	F4	F7	F10	F10.5
1863	0.2619	0.0106	0.0273	0.0499
4269	0.0466	0.0871	0.1975	0.0859
Everest	0.0213	0.0496	<0.0001	0.0228
Gallant	0.0013	0.0028	0.0504	0.0002
Grainfield	0.0018	0.0094	0.0164	0.0305
All	0.3364	0.1391	0.0007	0.0041

Table 2-7 Yield/CCCI 2017 r^2

Conclusions

This study found that in 2016, variety did not have a statistical impact on yield, however variety did have a statistical impact on protein and vegetative indices across all growth stages with the exception of NDVI during Feekes 4. This study also found that in 2017, variety did have a statistical impact on yield, protein and all vegetative indices across all growth stages. These findings were attributed to the varieties' physiological traits and how they interact with the environment. These variety traits are more

pronounced in high stress years than in favorable growing conditions. Generally, more deviation was identified across varieties when using vegetative indices utilizing red-edge. This was more pronounced in 2017, when foliar damages were present.

The findings of this research would indicate that variety physiological traits have an impact on yield, protein and vegetative indices readings. Due to this variety interaction, broad scale phenotyping across multiple varieties is possible, however this variation does present challenges for algorithm development. Further research will need to be conducted to determine what wheat varieties are similar enough to make cross variety comparisons using vegetative indices.

References

Allen, W. A., Gausman, H. W., Richardson, A. J., & Thomas, J. R. (1969). Interaction of isotropic light with a compact plant leaf. JOSA, 59(10), 1376–1379.

Asebedo, A. R., Adee, E., & Mengel, D. B. (n.d.). Development of Variable Rate Nitrogen Recommendation Algorithms to Enhance Yield and Nitrogen Use Efficiency in High Yielding Dryland and Irrigated Corn.

Barnes, E. M., Clarke, T. R., Richards, S. E., Colaizzi, P. D., Haberland, J., Kostrzewski, M., … Thompson, T. (2000). Coincident detection of crop water stress, nitrogen status and canopy density using ground based multispectral data. In Proceedings of the Fifth International Conference on Precision Agriculture, Bloomington, MN, USA (Vol. 1619).

Blackburn, G. A. (1998). Spectral indices for estimating photosynthetic pigment concentrations: a test using senescent tree leaves. *International Journal of Remote Sensing*, *19*(4), 657–675.

Carter, G. A. (1998). Reflectance wavebands and indices for remote estimation of photosynthesis and stomatal conductance in pine canopies. *Remote Sensing of Environment*, *63*(1), 61–72.

Daughtry, C. S. T., Walthall, C. L., Kim, M. S., De Colstoun, E. B., & McMurtrey Iii, J. E. (2000). Estimating corn leaf chlorophyll concentration from leaf and canopy reflectance. *Remote Sensing of Environment*, *74*(2), 229–239.

Elvidge, C. D., & Chen, Z. (1995). Comparison of broad-band and narrow-band red and near-infrared vegetation indices. *Remote Sensing of Environment*, *54*(1), 38–48.

Fitzgerald, G. J., Rodriguez, D., Christensen, L. K., Belford, R., Sadras, V. O., & Clarke, T. R. (2006). Spectral and thermal sensing for nitrogen and water status in rainfed and irrigated wheat environments. *Precision Agriculture*, *7*(4), 233–248.

Gates, D. M., Keegan, H. J., Schleter, J. C., & Weidner, V. R. (1965). Spectral properties of plants. *Applied Optics*, *4*(1), 11–20.

Gausman, H. W. (1974). Leaf reflectance of near-infrared. *Photogrammetric Engineering*, *40*(2).

Gausman, H. W. (1977). Reflectance of leaf components. *Remote Sensing of Environment*, *6*(1), 1–9.

Gitelson, A. A., & Merzlyak, M. N. (1996). Signature analysis of leaf reflectance spectra: algorithm development for remote sensing of chlorophyll. *Journal of Plant Physiology*, *148*(3–4), 494–500.

Jordan, C. F. (1969). Derivation of leaf-area index from quality of light on the forest floor. *Ecology*, *50*(4), 663–666.

Lorence, A. A. (2017). *Evaluation of optical sensor technologies to optimize winter wheat (Triticum aestivum L.) management* (Thesis). Kansas State University. Retrieved from http://krex.k-state.edu/dspace/handle/2097/38245

Pinter Jr, P. J., Jackson, R. D., Idso, S. B., & Reginato, R. J. (1981). Multidate spectral reflectance as predictors of yield in water stressed wheat and barley. *International Journal of Remote Sensing*, *2*(1), 43–48.

Rasmussen, J., Nielsen, J., Garcia-Ruiz, F., Christensen, S., & Streibig, J. C. (2013). Potential uses of small unmanned aircraft systems (UAS) in weed research. *Weed Research*, *53*(4), 242–248. https://doi.org/10.1111/wre.12026

RedEdge Manual > Specifications. (n.d.). Retrieved March 17, 2018, from http://support.micasense.com/hc/en-us/articles/225950667-RedEdge-Manual-Specifications

Rouse Jr, J. W. (1973). Monitoring the vernal advancement and retrogradation (green wave effect) of natural vegetation.

Stone, M. L., Solie, J. B., Raun, W. R., Whitney, R. W., Taylor, S. L., & Ringer, J. D. (1996). Use of spectral radiance for correcting in-season fertilizer nitrogen deficiencies in winter wheat. *Transactions of the ASAE*, *39*(5), 1623–1631.

Tarpley, L., Reddy, K. R., & Sassenrath-Cole, G. F. (2000). Reflectance indices with precision and accuracy in predicting cotton leaf nitrogen concentration. *Crop Science*, *40*(6), 1814–1819.

Thenkabail, P. S., Smith, R. B., & De Pauw, E. (2002). Evaluation of narrowband and broadband vegetation indices for determining optimal hyperspectral wavebands for agricultural crop characterization. *Photogrammetric Engineering and Remote Sensing*, *68*(6), 607–622.

Tucker, C. J., Holben, B. N., Elgin Jr, J. H., & McMurtrey III, J. E. (1980). Relationship of spectral data to grain yield variation. *Photogrammetric Engineering and Remote Sensing*, *46*(5), 657–666.

Wang, H. (2017). Crop assessment and monitoring using optical sensors. Retrieved from http://krex.k-state.edu/dspace/handle/2097/38224

Woolley, J. T. (1971). Reflectance and transmittance of light by leaves. *Plant Physiology*, *47*(5), 656–662.

Chapter 3 - Estimating Cattle Rectal Temperature Using Thermography

Abstract

In high stocking densities, infectious disease can spread rapidly. To control and contain disease, early identification and treatment is vital. Conventional techniques are time consuming and labor intensive. These factors have driven researchers to focus on the integration of thermography into animal wellness programs. This chapter focuses on determining if sUAS based thermography can be used to determine rectal temperature. Before conducting sUAS based thermographic readings, one must first identify the most ideal area on the animal to take thermographic readings. To conduct this research, 35 steers were identified and placed into a squeeze chute where rectal temperatures were recorded along with thermographic readings of the ocular regions, the muzzle and the forehead between the eyes. Thermographic data was captured using a 13mm FLIR VUE Pro R at six predetermined sensor locations, for consistency and repeatability. Raw data was processed using FLIR Tools software package, and regression analysis was conducted. This study shows moderate correlation between the ocular regions and rectal temperature, and no correlation with forehead or muzzle regions and rectal temperatures. More complex algorithms will need to be developed if absolute temperatures are to be predicted using thermography.

Introduction

In high stocking densities, the early detection and treatment of contagious disease is vital to controlling the spread of disease (Schaefer et al., 2004). However, conventional methods are

time consuming and logistically challenging, as most current methods require physical contact with the animal to perform invasive procedures, such as taking rectal temperatures, collecting blood samples or measuring respiratory and heart rate (Stewart, Stafford, Dowling, Schaefer, & Webster, 2008). The handling of animals to collect these invasive procedures may cause an anxiogenic response in the animals skewing the data collected (Soerensen & Pedersen, 2015). These factors have driven researchers to develop noninvasive remote sensing techniques to monitor animal health and welfare. Thermography is one such technique that is being used to detect animal health and welfare.

Infrared thermography works on the principle of Wien's Law that all bodies between -173°C and 2,727°C emit infrared radiation (Carlo, 1995). Infrared thermographic sensors are able to sense this infrared radiation and translate the incoming radiation into a visible form. Ground based thermographic sensors have been successfully used in several veterinarian health studies to detect illness in animals. Thermographic ocular readings of cattle have shown the ability to detect bovine viral diarrhea virus several days before convention clinical measurements (Schaefer et al., 2004). Ocular readings have also been utilized for early detection of respiratory disease in cattle (Schaefer et al., 2004). Early signs of foot lesions have also been detected with thermographic sensors, limiting lameness (Alsaaod, Schaefer, Büscher, & Steiner, 2015). The thermographic detection of foot lesions have even shown promise as a detector of foot and mouth disease (Rainwater-Lovett, Pacheco, Packer, & Rodriguez, 2009). The screening of cattle udders using thermographic sensors has shown the ability to detect early signs of mastitis and other disease (Berry, Kennedy, Scott, Kyle, & Schaefer, 2003; Colak et al., 2008; Hovinen et al., 2008).

Rational and objective

With all the proven benefits that infrared thermographic readings have exhibited, one must ask if these sensors could be incorporated into an sUAS platform to increase the mobility and usefulness of these sensors. The major challenge for sUAS based thermographic readings of cattle is identifying what location on the animal should thermographic readings be taken. Many researchers have focused on areas such as the coronary band and udder. These locations work well for ground based sensors, but are not a viable option for aerial based thermography as these locations are generally blocked by the animal's body when viewed from above. Therefore, one must look for other locations to measure body temperature. Due to the tendency to get unobstructed views of the cattle's heads during sUAS flights, this research has chosen to evaluate facial features on their correlation to rectal temperature. Four areas of interest were selected for this research, right and left ocular regions, forehead and muzzle.

Materials and Methods

Animals and experimental protocol

35 commercial steers were utilized for this study. These steers were housed in a feedlot setting with open access to water and were fed a diet consisting of 33.16% dry rolled corn, Supp 6.60%, alfalfa hay 5.32%, prairie hay 5.28% and WCGF-Sweet Bran 49.64%. For data collection, steers were brought into an indoor hydraulic squeeze chute, in a calm manner to help minimize anxiogenic responses. While in the chute, 12 thermographic readings were taken from each animal along with rectal temperature using GLA M750 digital thermometer.

Thermographic readings

Thermographic readings were taken using a 13mm FLIR VUE PRO R imager. This sensor was chosen, as it is commonly incorporated into sUAS platforms. The sensor is also radiometric, allowing each pixel to be assigned with a temperature value rather than a brightness value. For this experiment the sensor was mounted onto a tripod, as conducting a sUAS flight near the chute could have posed danger to both the animals and people conducting the research. Along with the FLIR VUE PRO R, the tripod also had a RGB monitor allowing researchers to accurately aim the thermographic sensor. Six sensor positions were marked on the floor allowing for repeated measurements (figure 3-1). Two pictures were taken at each camera location, with the animal's head in the center of the image. The thermographic sensor was calibrated using the FLIR UAS mobile application before the first photo at each location. Weather data for this calibration was acquired from an onsite weather station.

Interpolation of thermographic data

The collected raw thermographic data was first sorted to insure image quality. Images where the animal's eyes were closed or when the animal's facial features were obstructed were culled. The remaining raw data was imported into the FLIR tools desktop application where maximum temperature values were determined for each area of interest. From the side profile readings, a square encompassing the ocular region was drawn around the eye and maximum temperature values were calculated and recorded (figure 3-2). Frontal profile images had similar readings recorded on the animal's muzzle and forehead between the eyes (figure3-2). These measurements, along with rectal temperatures were tabulated into a spreadsheet and simple regression models were ran to determine correlation.

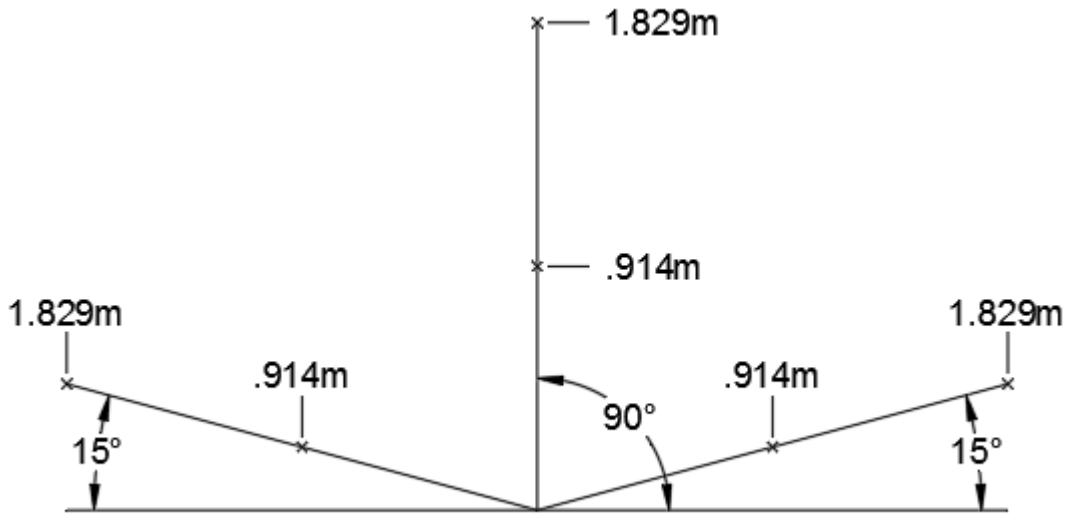

Figure 3-1 thermographic sensor positions

Figure 3-2 On animal thermographic reading locations

Results and Discussion

Results

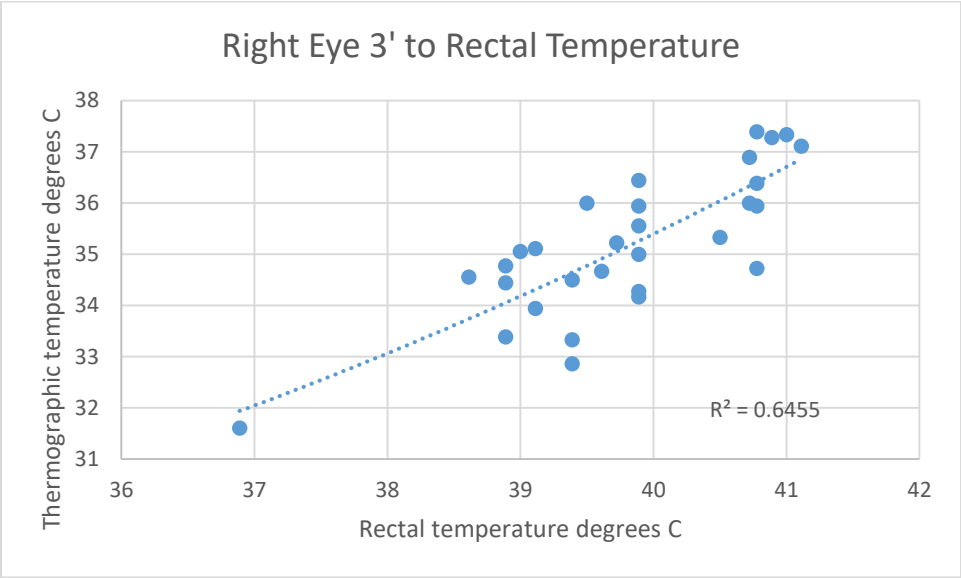

Figure 3-3 Right eye to rectal temperature, taken from sensor position A

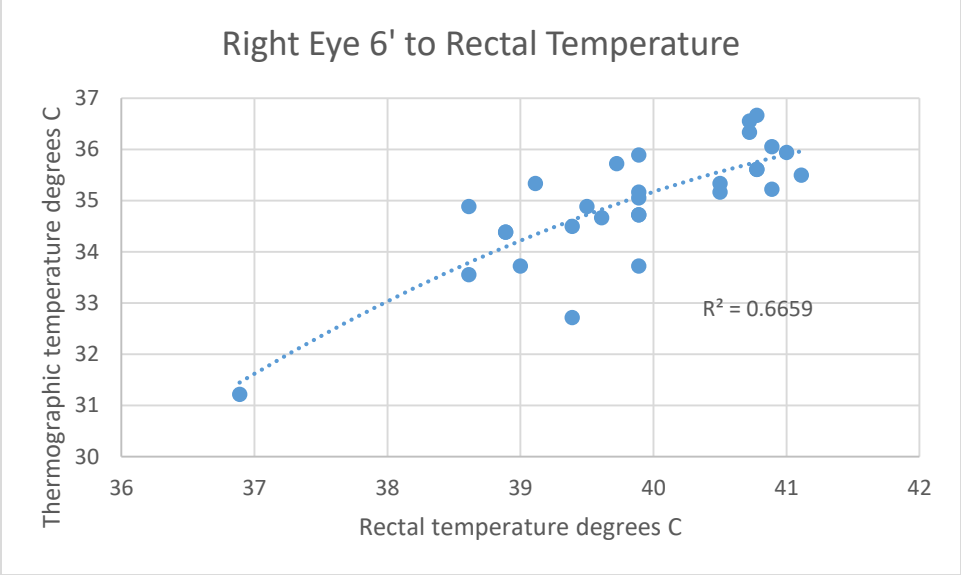

Figure 3-4 Right eye to rectal temperature, taken from sensor position B

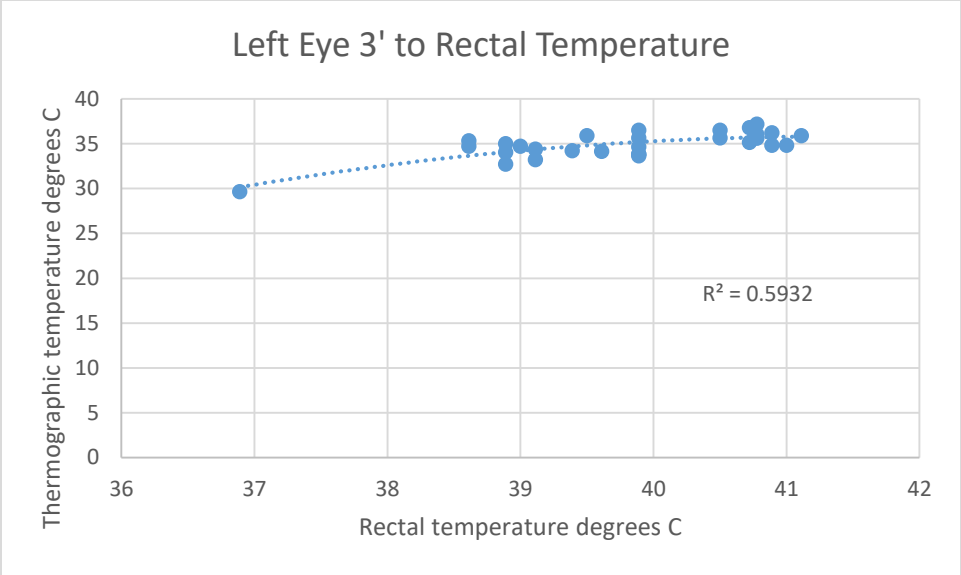

Figure 3-5 Left eye to rectal temperature, taken from sensor position E

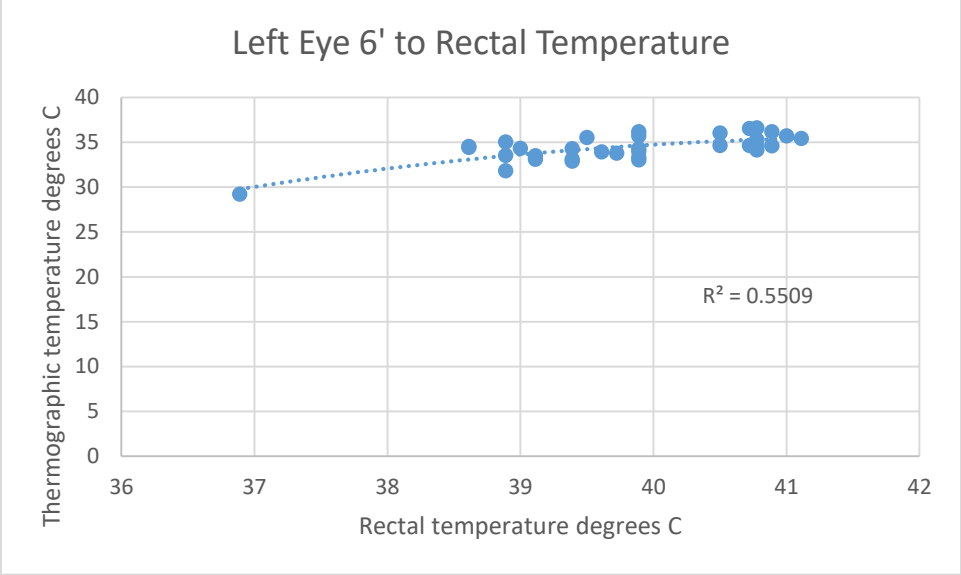

Figure 3-6 Left eye to rectal temperature, taken from sensor position F

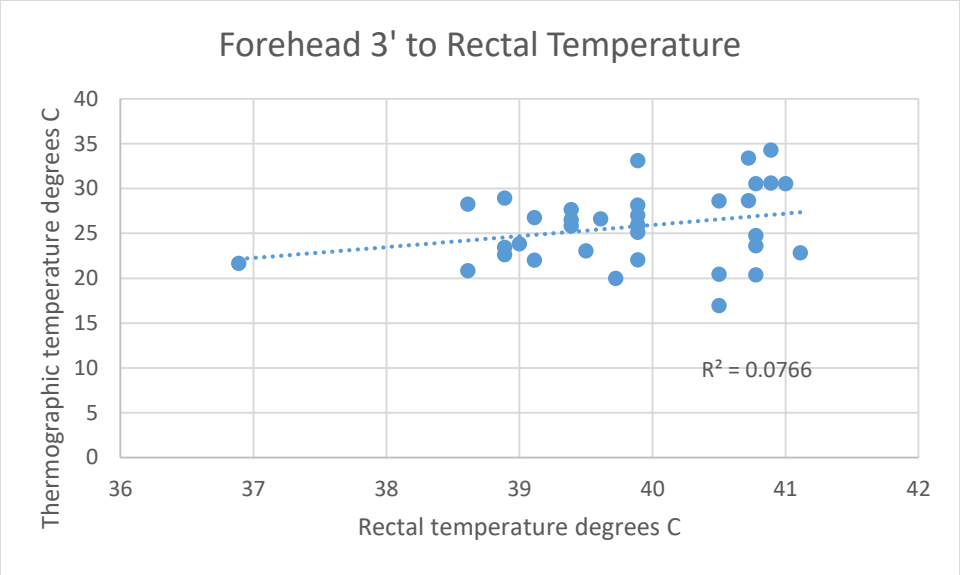

Figure 3-7 Forehead to rectal temperature, taken from sensor position C

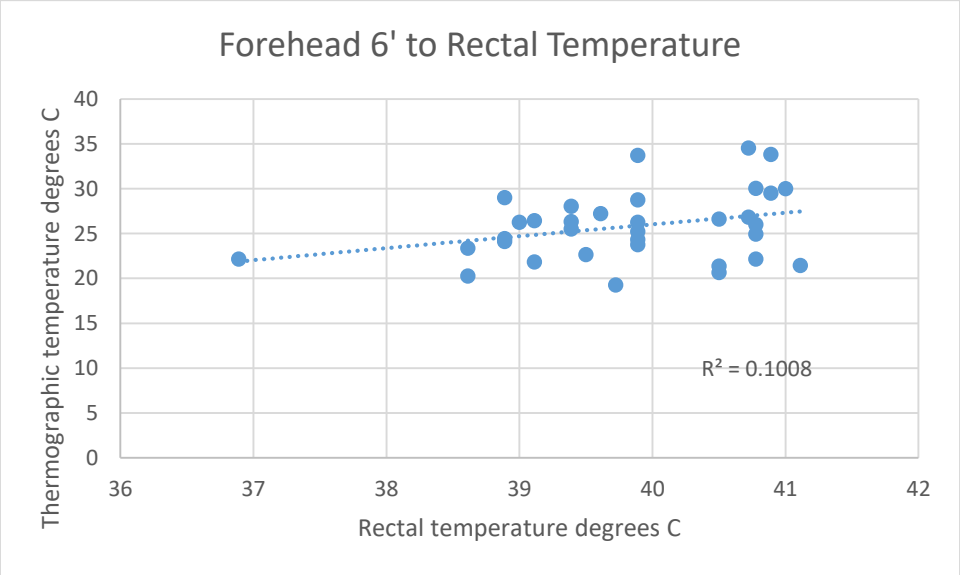

Figure 3-8 Forehead to rectal temperature, taken from sensor position D

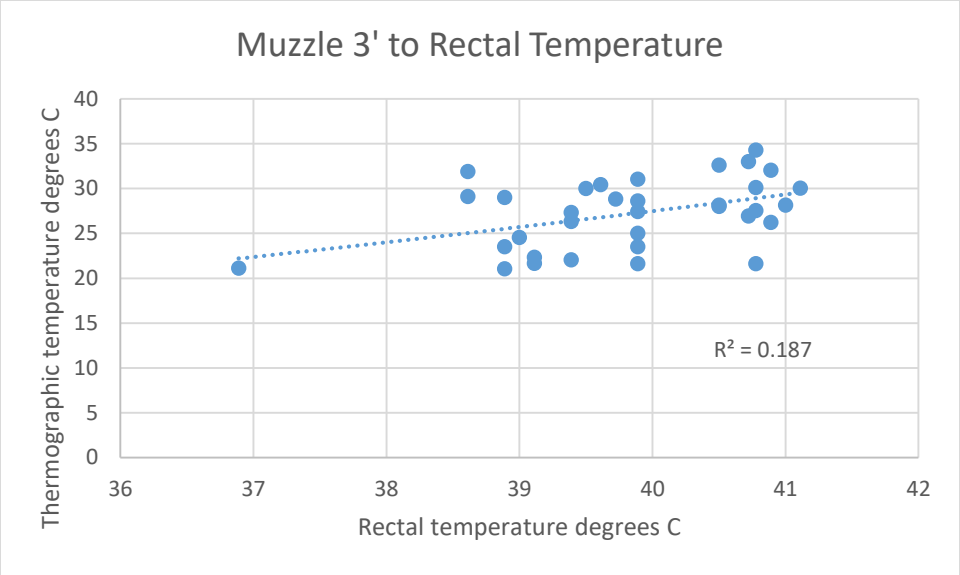

Figure 3-9 Muzzle to rectal temperature, taken from sensor position C

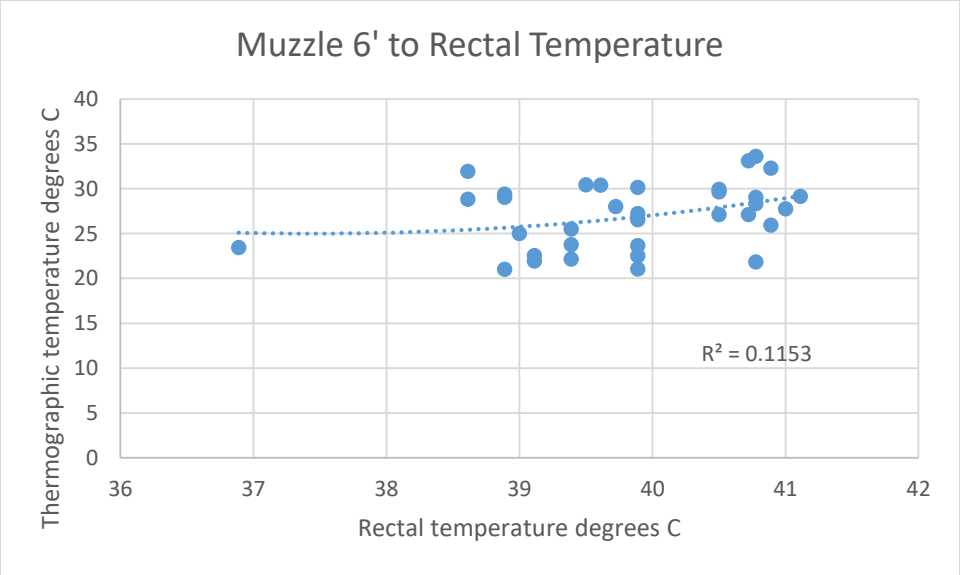

Discussion

The data shows that the ocular region of the face is the most favorable feature to predict rectal temperature. This research showed that ocular regions were statistically significant, whereas the muzzle and forehead were not statistically significant. This is expected, as ocular

regions have membranes in the tear duct that are less insulated, thus causing less variability leading to R^2 values as high as 0.6659. The animal's forehead showed the least correlation with an R^2 value of 0.0766 at 0.914 meters and 0.1008 at 1.829 meters. This is likely due to differences in hide and hair and their insulative properties. The muzzle also showed poor correlation with R^2 values of 0.187 at 0.914 meters and 0.1153 at 1.829 meters.

This research shows a higher correlation with the right eye than left eye to rectal temperature, however this is likely due to experimental design. While taking readings of the right eye at sensor positions A and B, the thermographic sensor was in shade cast by the building's door. In comparison, readings of the left eye at positions E and F, the sensor was not in the shade. These different lighting conditions likely explain the difference in correlation between right and left eyes.

Conclusions and Further Research

While this research showed correlation between ocular temperatures and rectal temperature, current correlation values are too low to accurately predict an animal's temperature. Muzzle and forehead thermographic readings show no statistical significance with rectal temperature. Therefore, one should focus thermographic readings on the ocular region of the face.

To explain the variation in animal's thermographic readings, more research will need to be conducted and algorithms developed. More accurate calibration methods will need to be devised, to capture differences in hair color and thickness, solar radiance, wind speed and target to sensor distance, if accurate thermal predictions are to be made.

While current capabilities are too low to accurately predict absolute internal temperature, current capabilities have been shown to be an early screening devise. One should also consider

formulating defined ranges of thermal readings to establish a threshold system, where animals could be designated as “acceptable” or unacceptable”. These animals deemed “unacceptable” could then be further screened with traditional clinical measures. This early screen could potentially increase profitability and decrease loss caused by illness and mortality.

References

Alsaaod, M., Schaefer, A. L., Büscher, W., & Steiner, A. (2015). The role of infrared thermography as a non-invasive tool for the detection of lameness in cattle. *Sensors*, *15*(6), 14513–14525.

Berry, R. J., Kennedy, A. D., Scott, S. L., Kyle, B. L., & Schaefer, A. L. (2003). Daily variation in the udder surface temperature of dairy cows measured by infrared thermography: Potential for mastitis detection. *Canadian Journal of Animal Science*, *83*(4), 687–693.

Carlo, A. D. (1995). Thermography and the possibilities for its applications in clinical and experimental dermatology. *Clinics in Dermatology*, *13*(4), 329–336. https://doi.org/10.1016/0738-081X(95)00073-O.

Colak, A., Polat, B., Okumus, Z., Kaya, M., Yanmaz, L. E., & Hayirli, A. (2008). Early Detection of Mastitis Using Infrared Thermography in Dairy Cows. *Journal of Dairy Science*, *91*(11), 4244–4248.

Hovinen, M., Siivonen, J., Taponen, S., Hänninen, L., Pastell, M., Aisla, A.-M., & Pyörälä, S. (2008). Detection of Clinical Mastitis with the Help of a Thermal Camera. *Journal of Dairy Science*, *91*(12), 4592–4598. https://doi.org/10.3168/jds.2008-1218

Rainwater-Lovett, K., Pacheco, J. M., Packer, C., & Rodriguez, L. L. (2009). Detection of foot-and-mouth disease virus infected cattle using infrared thermography. *The Veterinary Journal*, *180*(3), 317–324. https://doi.org/10.1016/j.tvjl.2008.01.003.

Schaefer, A. L., Cook, N., Tessaro, S. V., Deregt, D., Desroches, G., Dubeski, P. L., … Godson, D. L. (2004). Early detection and prediction of infection using infrared thermography. *Canadian Journal of Animal Science*, *84*(1), 73–80.

Soerensen, D. D., & Pedersen, L. J. (2015). Infrared skin temperature measurements for monitoring health in pigs: a review. *Acta Veterinaria Scandinavica*, *57*, 5. https://doi.org/10.1186/s13028-015-0094-2

Stewart, M., Stafford, K. J., Dowling, S. K., Schaefer, A. L., & Webster, J. R. (2008). Eye temperature and heart rate variability of calves disbudded with or without local anaesthetic. *Physiology & Behavior*, *93*(4), 789–797. https://doi.org/10.1016/j.physbeh.2007.11.044.